Biogeosciences, 12, 3197–3223, 2015
www.biogeosciences.net/12/3197/2015/
doi:10.5194/bg-12-3197-2015

Biogeosciences Open Access

Methane and carbon dioxide emissions from 40 lakes along a north–south latitudinal transect in Alaska

A. Sepulveda-Jauregui[1], K. M. Walter Anthony[1], K. Martinez-Cruz[1,2], S. Greene[3], and F. Thalasso[1,2]

[1]Water and Environmental Research Center, University of Alaska Fairbanks, P.O. Box 5860, 99775 Fairbanks, Alaska, USA
[2]Biotechnology and Bioengineering Department, Cinvestav, 07360 Mexico City, D. F., Mexico
[3]Department of Chemistry, The University of Chicago, 60637 Chicago, Illinois, USA

Correspondence to: K. M. Walter Anthony (kwalteranthony@alaska.edu)

Received: 20 July 2014 – Published in Biogeosciences Discuss.: 16 September 2014
Revised: 14 April 2015 – Accepted: 25 April 2015 – Published: 2 June 2015

Abstract. Uncertainties in the magnitude and seasonality of various gas emission modes, particularly among different lake types, limit our ability to estimate methane (CH_4) and carbon dioxide (CO_2) emissions from northern lakes. Here we assessed the relationship between CH_4 and CO_2 emission modes in 40 lakes along a latitudinal transect in Alaska to lakes' physicochemical properties and geographic characteristics, including permafrost soil type surrounding lakes. Emission modes included direct ebullition, diffusion, storage flux, and a newly identified ice-bubble storage (IBS) flux. We found that all lakes were net sources of atmospheric CH_4 and CO_2, but the climate warming impact of lake CH_4 emissions was 2 times higher than that of CO_2. Ebullition and diffusion were the dominant modes of CH_4 and CO_2 emissions, respectively. IBS, $\sim 10\,\%$ of total annual CH_4 emissions, is the release to the atmosphere of seasonally ice-trapped bubbles when lake ice confining bubbles begins to melt in spring. IBS, which has not been explicitly accounted for in regional studies, increased the estimate of springtime emissions from our study lakes by 320 %. Geographically, CH_4 emissions from stratified, mixotrophic interior Alaska thermokarst (thaw) lakes formed in icy, organic-rich yedoma permafrost soils were 6-fold higher than from non-yedoma lakes throughout the rest of Alaska. The relationship between CO_2 emissions and geographic parameters was weak, suggesting high variability among sources and sinks that regulate CO_2 emissions (e.g., catchment waters, pH equilibrium). Total CH_4 emission was correlated with concentrations of soluble reactive phosphorus and total nitrogen in lake water, Secchi depth, and lake area, with yedoma lakes having higher nutrient concentrations, shallower Secchi depth, and smaller lake areas. Our findings suggest that permafrost type plays important roles in determining CH_4 emissions from lakes by both supplying organic matter to methanogenesis directly from thawing permafrost and by enhancing nutrient availability to primary production, which can also fuel decomposition and methanogenesis.

1 Introduction

Lakes are an important source of atmospheric greenhouse gases, methane (CH_4), and carbon dioxide (CO_2) (Battin et al., 2009; Tranvik et al., 2009; Bastviken et al., 2011). In lakes, CH_4 is produced, consumed, and exchanged with the atmosphere in a different manner than CO_2. CH_4 is produced in anaerobic environments (mainly in sediments), while CO_2 in lakes originates from respiration throughout the water column and sediments, inflow of terrestrially derived dissolved inorganic carbon from surrounding watersheds, and photooxidation of dissolved organic carbon (DOC) (Graneli et al., 1996; Tranvik et al., 2009; Weyhenmeyer et al., 2012; Maberly et al., 2013). CO_2 is also formed in lakes by aerobic oxidation of CH_4, a process that can consume a significant fraction of CH_4 produced in lakes (Kankaala et al., 2006; Bastviken et al., 2008; Lofton et al., 2013). The ratio of CO_2 emissions versus carbon sequestration in northern lakes was found to be controlled by nitrate concentrations in lake water (Kortelainen et al., 2013). Meanwhile, CO_2 is consumed by photosynthesis and other autotrophic or chemical processes

(e.g., increasing alkalinity, photooxidation) that depend on pH and/or the availability of light (Madigan et al., 2009).

Despite recycling of CH_4 and CO_2 internally in lakes, a significant quantity of these greenhouse gases is released from lakes to the atmosphere (Cole et al., 2007). Most of Earth's lakes are located in northern high latitudes, overlapping the permafrost-dominated region (Downing et al., 2006; Smith et al., 2007; Grosse et al., 2013). It is estimated that CH_4 emission from lakes globally comprises about 16 % (71.6 Tg) of all human and natural atmospheric sources, and that northern lakes (> 55° N) contribute about 20 % of these emissions (13.6 Tg; Bastviken et al., 2011). In contrast, CO_2 emissions from northern lakes constitute approximately 43 % (1.2 Pg CO_2) of global emissions from lakes (Battin et al., 2009; Tranvik et al., 2009; Maberly et al., 2013). This disproportionality between the contribution of CH_4 and CO_2 emissions from northern lakes is not well understood, and may be due to numerous factors, including sensitivity of methanogenesis to temperature and lake trophic status (Tranvik et al., 2009; Ortiz-Llorente and Alvarez-Cobelas, 2012; Marotta et al., 2014) versus processes that control CO_2 availability (e.g., photosynthesis, inputs from terrestrial ecosystems, and organic matter mineralization) (Kling et al., 1991; Battin et al., 2009; Tranvik et al., 2009). Furthermore, lake CH_4 emission data are scarce relative to CO_2 data, particularly at high northern latitudes (Tranvik et al., 2009; Bastviken et al., 2011). Due to a disproportionately low number of northern high-latitude lakes represented in previous studies of global CH_4 emissions (Bastviken et al., 2011), and a paucity of studies that considered various modes of emission together, CH_4 and CO_2 emissions from northern high-latitude lakes are still poorly constrained.

Landscape diversity in Alaska provides a valuable opportunity to study CH_4 and CO_2 emission patterns from lakes as they relate to origin, climate, ecology, geology, and permafrost coverage. Across Arctic, continental, and transitional climate zones in Alaska, ecological habitats include Arctic, alpine, and forest tundra, and northern and southern boreal forests (Gregory-Eaves et al., 2000). The surficial geology in which Alaskan lakes are found varies primarily from fine-grain aeolian deposits; to coarser-grain coastal, glacial, fluvial, and volcanic deposits; to rubble and bedrock (Karlstrom et al., 1964; Arp and Jones, 2009). Alaska is also characterized by a variety of permafrost types (Fig. 1) ranging from isolated permafrost in south-central Alaska to continuous permafrost in northern Alaska (Jorgenson et al., 2008).

Within the context of permafrost soil organic carbon content, Alaskan lakes can be classified depending on whether they are surrounded by yedoma-type permafrost or non-yedoma substrates (Walter Anthony et al., 2012). Yedoma is typically thick (tens of meters), Pleistocene-aged loess-dominated permafrost sediment with high organic carbon (∼ 2 % by mass) and ice (50–90 % by volume) contents (Zimov et al., 2006). When yedoma thaws and ground ice melts, deep thermokarst (thaw) lakes with high CH_4 production potentials form (Zimov et al., 1997; Kanevskiy et al., 2011; Walter Anthony and Anthony, 2013). Some non-yedoma permafrost soils can also have high organic carbon and excess ice concentrations within several meters of the ground surface; however, these organic- and ice-rich permafrost horizons are typically thinner than yedoma deposits (Ping et al., 2008; Tarnocai et al., 2009). As a result, thermokarst lakes formed in non-yedoma permafrost soils are commonly shallower than yedoma lakes and have been shown to emit less CH_4 (West and Plug, 2008; Grosse et al., 2013; Walter Anthony and Anthony, 2013).

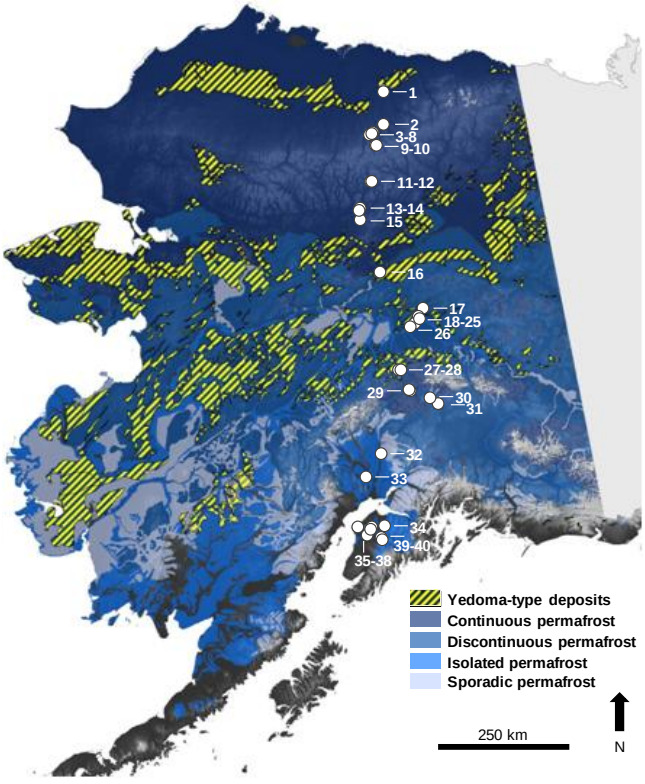

Figure 1. Locations of study lakes in Alaska (circles) plotted on the Alaska DEM hillshade raster. Information about the distribution of yedoma-type deposits (ice-rich silt containing deep thermokarst lakes) and permafrost is from Jorgenson et al. (2008) and Kanevskiy et al. (2011). The Alaska map is the National Elevation Dataset 30 m hillshade raster.

Estimating CH_4 and CO_2 emissions from northern high-latitude lakes, which are seasonally covered by ice, represents a difficult task because there are at least four emission pathways, all of which have not been consistently and simultaneously measured in the past: (1) direct ebullition, (2) diffusion, (3) storage flux, and a newly identified (4) ice-bubble storage (IBS) flux (Greene et al., 2014).

Ebullition (bubbling) has been observed as the dominant pathway of CH_4 emissions from many lakes (Casper et al., 2000; Bastviken et al., 2004; Walter et al., 2006). Since CH_4 is less soluble, high concentrations in interstitial sediment

water lead to bubble formation and their emission to the atmosphere. In contrast, CH_4 diffusion flux to the atmosphere is usually relatively low and occurs mainly in summer, when ice cover is absent. Due to much higher solubility, CO_2 tends to occur in low concentrations in ebullition bubbles, and instead escapes lakes predominately by diffusion (Abril et al., 2005).

During winter, ice formation on most northern lakes impedes gas emissions to the atmosphere. Dissolved CH_4 and CO_2 accumulate in the lake water column beneath the ice, resulting in gas "storage". Storage emissions occur when dissolved CH_4 and CO_2 are emitted by diffusion when the ice melts in spring, often enhanced by full or partial lake overturn (Michmerhuizen et al., 1996; Phelps et al., 1998; Bellido et al., 2009). Storage emissions also occur in some lakes in fall if lake overturn caused by falling temperature brings high concentrations of dissolved gases from the hypolimnion to the surface, resulting in rapid CH_4 and CO_2 emission by diffusion from the water column. Bastviken et al. (2004) coined the term "storage flux" when they considered it in regional lake emission estimates as a function of differences in water column CH_4 stocks before and after lake ice-out, CH_4 production, and CH_4 oxidation.

The fourth potential emission component involves CH_4 release to the atmosphere from seasonally ice-trapped ebullition bubbles in spring before the ice disappears. During winter, emission to the atmosphere of many bubbles rising from sediments is impeded by seasonal lake ice. When bubbles come to rest under the ice, they exchange gases with the water column (Greene et al., 2014). Some bubbles become sealed in ice as ice thickens downward. Due to the insulation property of gas bubbles, ice is locally thinner where bubbles are trapped, and bubbles usually stack in vertical columns separated by ice lenses of various thicknesses. As a result, when lake ice begins to melt in spring, bubble-rich patches of ice begin to locally degrade before the rest of the ice sheet. These ebullition bubbles previously sealed in and under ice are released to the atmosphere by an emission mode termed "ice-bubble storage" (IBS) (Greene et al., 2014). Ponded water on the lake-ice surface can accelerate the release of ice-trapped bubbles to the atmosphere and also provides the opportunity for visual observation of gas release from bubbles trapped by degrading ice (K. M. Walter Anthony, unpublished data, 2014). It should be noted that gas in small, tubular bubbles formed in lake ice by the exclusion of dissolved gases as ice freezes (Gow and Langston, 1977; Langer et al., 2015) is presumably released to the atmosphere when ice degrades as well; however, given the substantially lower concentration of CH_4 in these non-ebullition, freeze-out bubbles (usually < 0.01 % by volume; Boereboom et al., 2012), this mode of emission is relatively insignificant in comparison to the larger ebullition-sourced bubbles, in which CH_4 concentrations typically range from 40 to 90 % by volume (Martens et al., 1992; Semiletov et al., 1996; Walter Anthony et al., 2010).

Finally, it is important to understand how changes in nutrient availability and temperature influence CO_2 and CH_4 cycling in lakes. Increasing nutrients and temperature stimulates primary production and microbial decomposition of organic matter, which in turn consumes oxygen (O_2) and enhances anaerobic decay processes, particularly in sediments, where CH_4 and CO_2 are produced (Conrad et al., 2010). Aerobic CH_4 oxidation is controlled directly by O_2 and CH_4 concentrations and temperature (Utsumi et al., 1998; Bastviken et al., 2002; Borrel et al., 2011) and indirectly by nutrient availability (Dzyuban et al., 2010). Measurements of O_2 and CH_4 concentrations in lakes are essential for assessing global carbon cycling, and in this framework, correlating both parameters in situ has been promoted as an indirect means of assessing CH_4 oxidation by methanotrophs (Bastviken et al., 2004; Guerin and Abril, 2007; Sepulveda-Jauregui et al., 2012).

In this study we assessed the relationships between measured CH_4 and CO_2 emission modes in 40 lakes along a north–south Alaska transect to the lakes' physicochemical properties and geographic characteristics. Our goal was to assess the magnitude, variability, and seasonality of individual modes of emission, particularly among the wide range of geographic lake settings in Alaska.

2 Materials and methods

2.1 Study lakes and permafrost zones

We sampled water from 40 Alaskan lakes during open-water conditions in June–July 2011 and 2012 (Fig. 1) and from 26 of the lakes toward the end of the winter ice-cover period in March–April 2011. Measurements were usually made during daylight hours between 10:00 and 18:00 LT. Our study lakes were located near the road system along a north–south transect in Alaska that spans a variety of geographic and limnological settings, described previously by Gregory-Eaves et al. (2000), Jorgenson et al. (2008), and Walter Anthony et al. (2012). Our study lakes occupied three general climatic/permafrost zones: (1) the northern study area (66–70° N, Arctic climate/continuous permafrost), (2) the interior study area (64–66° N, continental climate/discontinuous permafrost), and the southern study area (60–64° N, transitional climate/sporadic and isolated permafrost) (Gregory-Eaves et al., 2000; Jorgenson et al., 2008). Additionally, we distinguished yedoma-type thermokarst lakes as those formed in yedoma permafrost with active, ongoing thermokarst activity from non-yedoma-type lakes, which were lakes occurring in other non-yedoma deposits in permafrost and non-permafrost soils (Fig. 1). Lake names, sizes, geographic characteristics, and limnological properties are shown in Table 1.

Table 1. Lake physical and chemical properties from 40 Alaskan lakes. *N* – lake number; * indicates informal lake names, and the A number refers to lake identification numbers used by Gregory Eaves et al. (2000) for study of the same lakes; Y/NY[a,b] – permafrost soil type as yedoma or non-yedoma; TSI[c] – trophic state index; EC[d] – ecozonal categories; Lat – latitude; Long – longitude; DN[e] – sedimentary deposit name; MD – maximum known depth; A – area; SecD – Secchi depth. *T* (Win) – winter temperature; *T* (Sum) – summer temperature; pH (Win) – winter pH; pH (Sum) – summer pH; ORP (Win) – winter redox potential average; ORP (Sum) – summer redox potential; Chl *a* – summer surface chlorophyll *a*. SRP – soluble reactive phosphorus; NO_3^- – nitrate; SO_4^{2-} – sulfate; TOC – total organic carbon; TN – total nitrogen are from 1 m depth, except data summarized from other investigators[g,h]. TOCS – total organic carbon in surface sediments; TNS – total nitrogen in surface sediments. Error terms are the standard deviation. ND indicates not determined; CF indicates lake completely frozen; "<" indicates below detection limit; "–" indicates no standard deviation due a sample size of 1.

N	Name	Y/NY[a,b]	TSI[c]	EC[d]	Lat (° N)	Long (° W)	DN[e]	MD (m)	A (km^2)	SecD (m)	*T* (Win) (°C)	*T* (Sum) (°C)
1	Big Sky* A31	NY	O	ArT	69.581	148.639	ES	2.2	0.349	1.30	0.7 ± 0.2	15.7 ± 0.9
2	Dragon's Pond* A33	NY	O	ArT	68.795	148.843	GF	1.5	0.010	1.30	$2.4^{f} \pm 2.2$	18.4 ± 0.9
3	GTH 112	NY	Mx	ArT	68.672	149.249	GF	4.8	0.025	0.80	$2.6^{f} \pm 1.1$	11.7 ± 3.8
4	NE2	NY	O	ArT	68.647	149.582	GMD	2.7	0.067	2.70	0.4 ± 0.6	15.3 ± 0.6
5	E6	NY	O	ArT	68.643	149.440	GMD	2.6	0.027	2.60	$3.3^{f} \pm 1.5$	15.8 ± 1.0
6	E5 Oil Spill A30	NY	O	ArT	68.642	149.458	GMD	11.9	0.116	3.10	$2.8^{f} \pm 1.3$	10.8 ± 4.2
7	Toolik A28	NY	UO	ArT	68.632	149.605	GMD	24.1	1.449	3.31	2.2 ± 1.1	10.3 ± 4.1
8	E1	NY	UO	ArT	68.626	149.555	GMD	6.4	0.026	2.55	2.4 ± 0.8	12.4 ± 3.7
9	Autumn* A35	NY	UO	ArT	68.462	149.393	GMD	7.5	0.057	4.51	$0.45^{f} \pm 4.4$	13.5 ± 1.9
10	Julieta* A27	NY	UO	ArT	68.447	149.369	GMD	7.0	0.051	3.40	$-1.4^{f} \pm 2.0$	14.3 ± 1.2
11	El Fuego* A36	NY	UO	FoT	67.666	149.716	GMD	2.5	0.057	2.71	$2.9^{f} \pm 4.5$	15.7 ± 1.2
12	Jonas* A26	NY	UO	FoT	67.647	149.722	GMD	4.2	0.170	0.95	-0.2 ± 0.0	14.2 ± 4.8
13	Augustine Zoli* A25	NY	O	FoT	67.138	150.349	F	3.0	0.069	1.12	ND	17.3 ± 1.7
14	Ping*	NY	UO	FoT	67.136	150.370	F	1.4	0.102	1.08	0.1 ± 0.3	18.5 ± 1.7
15	Grayling A24	NY	O	FoT	66.954	150.393	MAC	1.8	0.401	1.80	0.4 ± 0.1	17.0 ± 0.8
16	Eugenia*	Y	Mx	FoT	65.834	149.631	ES	3.3	0.027	0.70	0.5 ± 0.7	17.0 ± 4.0
17	Vault*	Y	Mx	NBF	65.029	147.699	MAC	4.6	0.003	1.00	0.3 ± 0.3	9.5 ± 7.7
18	Goldstream*	Y	Mx	NBF	64.916	147.847	E	3.3	0.010	1.00	1.5 ± 1.5	9.3 ± 6.9
19	Doughnut*[a]	NY	O	NBF	64.899	147.908	E	3.8	0.034	1.59	0.7 ± 0.8	22.2 ± 2.2
20	Killarney*	Y	Mx	NBF	64.870	147.901	E	2.1	0.008	0.50	0.6 ± 0.7	7.8 ± 4.5
21	Smith A13[a]	NY	Mx	NBF	64.865	147.868	E	4.4	0.094	0.50	0.5 ± 0.7	19.0 ± 1.7
22	Stevens Pond*	Y	Mx	NBF	64.863	147.871	E	1.1	0.002	0.50	CF	17.6 ± 1.6
23	Duece A2	Y	Mx	NBF	64.863	147.942	E	6.0	0.023	0.79	0.9 ± 0.6	11.4 ± 7.0
24	Ace A1	Y	Mx	NBF	64.862	147.937	E	9.0	0.077	1.26	2.9 ± 0.9	11.6 ± 6.3
25	Rosie Creek*	Y	Mx	NBF	64.770	148.079	E	3.7	0.004	1.46	0.0 ± 0.3	11.9 ± 2.4
26	Monasta A37[a]	NY	Mx	NBF	64.741	148.276	MAC	5.6	0.005	0.43	ND	8.8 ± 5.6
27	91 Lake*	NY	O	NBF	63.848	148.973	F	0.5	0.066	1.40	ND	15.3 ± 0.7
28	Otto	NY	O	FoT	63.842	149.037	GMD	3.1	0.515	1.60	1.6 ± 1.3	12.0 ± 6.4
29	Floatplane* A16	NY	O	FoT	63.394	148.670	GL	5.0	0.103	1.20	$3.9^{f} \pm 1.5$	13.1 ± 1.3
30	Nutella* A39	NY	O	AlT	63.215	147.678	I	9.4	0.020	3.10	$3.4^{f} \pm 1.1$	10.2 ± 3.4
31	Swampbuggy A18	NY	O	FoT	63.055	147.421	GL	4.9	0.142	1.20	$3.2^{f} \pm 2.3$	13.7 ± 0.4
32	Montana A40	NY	O	SBF	62.143	150.048	F	9.0	0.300	2.80	0.8 ± 0.7	16.2 ± 2.4
33	Rainbow Shore* A41	NY	M	SBF	61.694	150.089	GL	11.5	0.575	2.00	0.9 ± 1.0	17.2 ± 1.8
34	Big Merganser A49	NY	O	SBF	60.726	150.644	GL	24.2	0.210	2.00	2.9 ± 1.3	14.4 ± 4.7
35	Rainbow A48	NY	UO	SBF	60.719	150.808	GMD	5.5	0.630	3.00	1.7 ± 1.6	14.8 ± 5.6
36	Dolly Varden A47	NY	UO	SBF	60.704	150.787	GL	30.0	1.074	11.00	2.5 ± 0.2	17.1 ± 0.6
37	Abandoned Cabin* A50	NY	O	SBF	60.696	151.315	GL	3.0	0.031	3.00	$1.9^{f} \pm 1.6$	17.4 ± 1.7
38	Scout A46	NY	O	SBF	60.533	150.843	GL	6.3	0.384	4.00	0.7 ± 0.7	16.4 ± 1.7
39	Engineer A45	NY	O	SBF	60.478	150.323	GMD	3.9	0.909	1.60	0.4 ± 0.6	16.4 ± 1.2
40	Lower Ohmer A44	NY	O	SBF	60.456	150.317	GMD	28.0	0.471	2.70	$3.6^{f} \pm 0.5$	11.6 ± 3.7
	Yedoma[i]	–	–	–	–	–	–	4.2^{k}	0.022^{k}	0.82^{k}	$1.1^{k,n} \pm 1.0$	$11.3^{k} \pm 4.5$
	Non-yedoma[j]	–	–	–	–	–	–	7.6^{k}	0.267^{l}	2.39^{l}	$1.6^{k,o} \pm 1.3$	$14.9^{l,p} \pm 3.0$

Table 1. Continued.

N	Name	pH (Win)	pH (Sum)	ORP (Win) (mV)	ORP (Sum) (mV)	Chl *a* ($\mu g\,L^{-1}$)	SRP ($\mu g\,P\,L^{-1}$)	NO_3^- ($mg\,NO_3^-$-$N\,L^{-1}$)
1	Big Sky* A31	7.0 ± 0.0	8.8 ± 0.7	102 ± 18	254 ± 78	2.6 ± 3.3	4.2[g]	< 0.01
2	Dragon's Pond* A33	ND	7.7 ± 0.5	ND	304 ± 78	4.7 ± 4.2	5.9[g]	ND
3	GTH 112	ND	7.2 ± 0.7	ND	264 ± 69	45.9 ± 7.4	ND	< 0.01
4	NE2	6.6 ± 0.1	7.9 ± 0.6	322 ± 17	299 ± 66	3.7 ± 4.6	1.3[h]	ND
5	E6	ND	7.7 ± 0.7	ND	272 ± 80	5.9 ± 6.2	1.1[h]	ND
6	E5 Oil Spill A30	ND	7.1 ± 0.8	ND	322 ± 64	13.5 ± 2.9	1.8[h]	ND
7	Toolik A28	6.9 ± 0.1	7.9 ± 0.8	303 ± 32	308 ± 75	1.5 ± 0.4	1.6[h]	< 0.01
8	E1	7.0 ± 0.1	9.1 ± 0.4	283 ± 58	231 ± 71	1.3[g] ± –	1.1[h]	< 0.01
9	Autumn* A35	ND	8.2 ± 0.6	ND	303 ± 45	2.9 ± 2.4	2.8[g]	ND
10	Julieta* A27	ND	8.5 ± 0.6	ND	318 ± 34	3.4 ± 3.8	3.6[g]	< 0.01
11	El Fuego* A36	ND	8.8 ± 0.4	ND	271 ± 50	1.2 ± 0.1	ND	ND
12	Jonas* A26	8.2 ± 0.0	8.5 ± 0.6	23 ± 4	250 ± 119	1.0 ± 0.0	6.6[g]	0.02
13	Augustine Zoli* A25	ND	8.7 ± 0.6	ND	259 ± 80	10.1 ± 11.4	9.8[g]	< 0.01
14	Ping*	5.9 ± 0.0	6.9 ± 0.2	211 ± 6	303 ± 21	22.4 ± 0.0	ND	< 0.01
15	Grayling A24	6.3 ± 0.0	7.6 ± 0.5	119 ± 4	323 ± 66	20.7 ± 20.5	5.3	< 0.01
16	Eugenia*	6.3 ± 0.0	7.0 ± 0.3	118 ± 9	314 ± 45	41.9 ± 2.4	ND	< 0.01
17	Vault*	7.7 ± 0.7	8.6 ± 0.8	75 ± 62	156 ± 87	35.0 ± 15.0	ND	ND
18	Goldstream*	7.4 ± 0.6	7.9 ± 0.7	117 ± 118	216 ± 134	31.0 ± 14.5	9.7	0.01
19	Doughnut*[a]	6.8 ± 0.1	7.7 ± 0.6	189 ± 56	254 ± 77	113.4 ± 0.0	ND	ND
20	Killarney*	7.0 ± 0.1	7.6 ± 0.7	66 ± 45	316 ± 99	ND	10.2	0.01
21	Smith A13[a]	6.5 ± 0.0	8.3 ± 1.1	98 ± 16	187 ± 99	44.7 ± 0.6	16.2[g]	< 0.01
22	Stevens Pond*	CF	8.4 ± 1.7	CF	212 ± 136	43.7 ± 13.4	CF	CF
23	Duece A2	7.2 ± 0.0	9.2 ± 0.4	58 ± 10	-20 ± 94	1.5[g] ± –	60.2[g]	0.32
24	Ace A1	7.1 ± 0.0	8.1 ± 1.0	68 ± 15	116 ± 161	54.0[g] ± –	31.5[g]	0.02
25	Rosie Creek*	7.1 ± 0.0	8.1 ± 1.0	33 ± 19	245 ± 127	45.3 ± 1.9	ND	ND
26	Monasta A37[a]	ND	6.3 ± 0.1	ND	160 ± 119	ND	24.9[g]	ND
27	91 Lake*	ND	8.2 ± 0.0	ND	351 ± 25	ND	ND	ND
28	Otto	7.1 ± 0.1	7.8 ± 0.5	120 ± 141	260 ± 59	8.2 ± 11.6	9.8	0.01
29	Floatplane* A16	ND	8.1 ± 0.5	ND	349 ± 25	27.1 ± 1.3	4.3[g]	ND
30	Nutella* A39	ND	7.2 ± 0.3	ND	384 ± 20	13.6 ± 1.4	3.3[g]	ND
31	Swampbuggy A18	ND	7.3 ± 0.0	ND	362 ± 1	7.9 ± 0.9	4.7[g]	ND
32	Montana A40	6.1 ± 0.0	7.1 ± 0.4	290 ± 31	329 ± 61	9.5 ± 0.4	2.2[g]	< 0.01
33	Rainbow Shore* A41	6.5 ± 0.3	7.9 ± 0.4	289 ± 12	305 ± 49	7.2 ± 0.9	4.7[g]	0.02
34	Big Merganser A49	6.4 ± 0.4	7.1 ± 0.3	321 ± 38	325 ± 49	7.4 ± 1.1	4.4[g]	< 0.01
35	Rainbow A48	7.0 ± 0.0	7.7 ± 0.6	241 ± 62	289 ± 85	12.6 ± 0.4	4.8[g]	< 0.01
36	Dolly Varden A47	ND	7.1 ± 0.3	ND	282 ± 22	3.7 ± 0.5	2.1[g]	< 0.01
37	Abandoned Cabin* A50	6.0 ± 0.5	6.3 ± 0.2	299 ± 113	338 ± 33	10.2 ± 1.1	2.3[g]	0.04
38	Scout A46	6.3 ± 0.4	7.0 ± 0.4	290 ± 36	347 ± 25	10.9 ± 0.4	4.7[g]	0.01
39	Engineer A45	6.7 ± 0.3	7.8 ± 0.4	273 ± 31	267 ± 43	7.0 ± 0.2	7.5[g]	< 0.01
40	Lower Ohmer A44	ND	7.5 ± 0.5	ND	379 ± 50	9.9 ± 0.5	1.8[g]	< 0.01
	Yedoma[i]	$7.1^{k,m} \pm 0.5$	$8.2^{k,m} \pm 0.9$	$84^{k,m} \pm 27$	$187^{k,m} \pm 118$	$34.5^{k} \pm 18.0$	27.9[k]	0.09[k]
	Non-yedoma[j]	$6.7^{l,o} \pm 0.5$	$7.7^{k,p} \pm 0.7$	$222^{l,o} \pm 95$	$295^{l,p} \pm 51$	$14.5^{l} \pm 21.8$	5.3[l]	0.02[k]

Table 1. Continued.

N	Name	SO_4^{2-} ($mg\,SO_4^{2-}$-$S\,L^{-1}$)	TOC ($mg\,L^{-1}$)	TN ($mg\,L^{-1}$)	TOCS (%)	TNS (%)
1	Big Sky* A31	< 0.04	16.48	1.3	1.8 ± 0.0	1.5 ± 0.3
2	Dragon's Pond* A33	6.20[g]	16.98	3.2	6.2 ± 0.8	2.2 ± 0.3
3	GTH 112	0.51	ND	ND	ND	ND
4	NE2	ND	0.93	0.2	2.9 ± 0.5	1.1 ± 0.2
5	E6	ND	ND	ND	3.5 ± 0.5	1.4 ± 0.1
6	E5 Oil Spill A30	< 0.04	ND	0.2[g]	8.1 ± 0.1	0.7 ± 0.0
7	Toolik A28	< 0.04	0.70	0.2	7.8 ± 1.3	0.8 ± 0.2
8	E1	< 0.04	0.18	0.2	ND	ND
9	Autumn* A35	5.30[g]	3.66	0.4	ND	ND
10	Julieta* A27	< 0.04	0.71	0.3[g]	0.8 ± 0.8	0.4 ± 0.2
11	El Fuego* A36	40.40[g]	ND	0.4	1.1 ± 0.2	0.5 ± 0.1
12	Jonas* A26	0.25	0.89	0.7	2.9 ± 2.2	1.1 ± 0.8
13	Augustine Zoli* A25	< 0.04	4.42	0.9	3.0 ± 0.4	1.1 ± 0.1
14	Ping*	0.18	12.38	0.9	ND	ND
15	Grayling A24	0.86	8.34	1.0	7.3 ± 1.8	0.3 ± 0.1
16	Eugenia*	< 0.04	16.51	0.8	22.0 ± 0.3	ND
17	Vault*	ND	ND	ND	8.0 ± 1.2	ND
18	Goldstream*	0.30	45.30	3.0	4.2 ± 0.6	ND
19	Doughnut*[a]	ND	ND	ND	24.0 ± 2.2	ND
20	Killarney*	0.01	18.12	2.3	3.5 ± 2.5	0.2 ± 0.1
21	Smith A13[a]	11.60	ND	1.3[g]	ND	ND
22	Stevens Pond*	CF	CF	CF	CF	CF
23	Duece A2	1.10	ND	2.4[g]	5.0 ± 0.7	1.8 ± 0.7
24	Ace A1	0.34	ND	1.3[g]	2.6 ± 2.5	1.0 ± 0.9
25	Rosie Creek*	ND	ND	ND	ND	ND
26	Monasta A37[a]	ND	58.80[g]	2.2[g]	ND	ND
27	91 Lake*	ND	ND	ND	ND	ND
28	Otto	0.20	3.63	0.8	8.8 ± 1.3	ND
29	Floatplane* A16	ND	ND	0.5[g]	ND	ND
30	Nutella* A39	ND	ND	0.3[g]	ND	ND
31	Swampbuggy A18	ND	ND	0.3[g]	ND	ND
32	Montana A40	< 0.04	0.16	0.3	ND	ND
33	Rainbow Shore* A41	0.33	52.20	0.1	38.8 ± 15.2	ND
34	Big Merganser A49	12.32	2.38	0.3	ND	ND
35	Rainbow A48	2.30	1.05	0.2	ND	ND
36	Dolly Varden A47	1.70	ND	0.2[g]	6.2 ± 0.7	ND
37	Abandoned Cabin* A50	0.76	ND	0.3[g]	25.7 ± 0.4	ND
38	Scout A46	0.78	2.58	0.4	23.0 ± 0.1	ND
39	Engineer A45	< 0.04	5.71	0.6	7.6 ± 1.2	ND
40	Lower Ohmer A44	2.50	ND	0.3[g]	ND	ND
	Yedoma[i]	0.44[k]	26.6[k]	2.0[k]	7.6[k] ± 7.3	1.0[k] ± 0.8
	Non-yedoma[j]	5.39[k]	10.1[l]	0.6[l]	10.0[k] ± 10.6	1.0[k] ± 0.6

[a] Doughnut Lake, a partially drained lake (uncalibrated ^{14}C age 1190 ± 20 yr BP, measured on outer wood of an in situ, dead tree near the lake center); Smith Lake, and Monasta Lake were included in the non-yedoma lake classification. While Doughnut and Monasta lakes likely formed in yedoma permafrost originally, following partial drainage events, they no longer appear to be influenced by active yedoma thaw along the margin. Smith Lake is thought to have formed as part of a previous river drainage network (V. Alexander, personal communication, 2011).
[b] Permafrost soil type: Y – yedoma; NY – non-yedoma.
[c] Trophic state index: UO – ultraoligotrophic; O – oligotrophic; M – mesotrophic; E – eutrophic; Mx – mixotrophic.
[d] Ecozonal categories according to Gregory Eaves et al. (2000): ArT – Arctic tundra; AlT – alpine tundra; FoT – forest tundra; NBF – northern boreal forest; SBF – southern boreal forest.
[e] Deposit name: ES – eolian silt; GF – glaciofluvial; GMD – old glacial moraines and drift; F – fluvial; MAC – mountain alluvium and colluvium; E – eolian; GL – glaciolacustrine (Jorgenson et al., 2008).
[f] Winter (October–April) temperature average from HOBO measurements.
[g] Data from Gregory Eaves et al. (2000).
[h] Data from Giblin et al. (2009); water-column average.
[i] Average from yedoma lakes (lake #25 excluded).
[j] Average from non-yedoma lakes.
[k,l] Different letters indicate a significant difference between yedoma and non-yedoma means.
[m,n] Different letters indicate a significant difference between summer and winter means in yedoma lakes for temperature, pH and ORP (Mann–Whitney *U* test).
[o,p] Different letters indicate a significant difference between summer and winter means in non-yedoma lakes for temperature, pH and ORP (Mann–Whitney *U* test).

2.2 Water-dissolved CH_4, CO_2, and O_2

Sampling of lake water was done offshore and usually near the center of each lake at one to nine distributed depths throughout the water column for dissolved CH_4 and CO_2 concentrations and at 0.5 m depth intervals for O_2 concentrations during winter and summer. In lakes shallower than 1 m we sampled only one depth within 25 cm of the lake bottom. In the field we measured CH_4 concentration via the headspace equilibration tunable diode laser spectroscopy (HE-TDLAS) method (Sepulveda-Jauregui et al., 2012) using a GasFinder 2.0 (Boreal Laser Inc., Edmonton, Canada; Appendix A1). Additionally, we determined concentrations of headspace CH_4 and CO_2 in bottles of lake water in the laboratory following Kling (2010) using a GC-2014 gas chromatograph (Shimadzu, Addison, Illinois, USA) equipped with a flame ionization detector and a PLOT alumina column (detector temperature 250 °C, oven 40 °C, high-purity helium as carrier gas). Strong correlation between the GasFinder and bottle headspace methods was reported previously by Sepulveda-Jauregui et al. (2012). Dissolved O_2 concentrations were measured in the field with a luminescence sensor connected to a calibrated multiparametric probe Hydrolab DataSonde (Hach LDO, Loveland, Colorado, USA).

2.3 CH_4 and CO_2 diffusion flux

We estimated the diffusion flux of CH_4 and CO_2 ($g\,m^{-2}\,yr^{-1}$) based on the once per summer measurement of dissolved CO_2 and CH_4 in surface water from each lake and extrapolating results to the summertime open-water period. We applied Fick's law to our measurements of dissolved CO_2 and CH_4 in surface water following the boundary layer method of Kling et al. (1992):

$$\text{Diffusion flux} = T \times D \times z^{-1} \times (C_w - C_{eq}), \quad (1)$$

where T is the conversion factor from seconds to years (31 536 000); D is the molecular diffusivity of CH_4 or CO_2 ($m^2\,s^{-1}$) following Kling et al. (1992); z (m) is the thickness of the surface boundary layer, assumed to be 200 µm as an average for Alaskan lakes following Kling et al. (1992); C_w is the measured gas concentration at the bottom of the boundary layer ($g\,m^{-3}$); and C_{eq} is the equilibrium gas concentration in surface lake water ($g\,m^{-3}$) exposed to the atmosphere at the top of the boundary layer. We calculated C_w and C_{eq} using measured surface water temperatures, Henry's law constants, and temperature dependence constants for CH_4 and CO_2, respectively (NIST, 2011). We acknowledge that wind speed and heat exchange vary over different timescales and that they have a large effect on the gas exchange coefficient (Cole and Caraco, 1998; Tedford et al., 2014) and thus on the relative importance of diffusion emission from lakes. However, due to lacking wind speed and heat exchange data for our study lakes, our calculations are based on the assumption of a constant gas exchange coefficient derived from averaged wind speed values from lakes in our northern tundra study region (Kling et al., 1992). Because many of our study lakes are surrounded by trees, the average wind speed at these lakes during the open-water periods is likely more similar to that of the low-wind Mirror Lake, studied by Cole and Caraco (1998). On one lake, Goldstream Lake (forested, interior Alaska), where we had higher temporal resolution data for surface-water-dissolved CH_4 concentrations (Greene et al., 2014) during the open-water summer period, we explored the effect of using the average value of the exchange coefficient from Cole and Caraco (1998) instead of Kling et al. (1992) and found that the exchange coefficient calculated from the boundary layer thickness of Kling et al. (1992) differed by 2 % from that from Cole and Caraco (1998).

2.4 Storage flux

To estimate storage flux, dissolved CH_4 and CO_2 profiles were measured in spring before the ice began to melt and in summer during ice-free conditions. We multiplied the average concentration of dissolved CH_4 and CO_2 measured in samples collected from distributed depths in the water column by the height of the unfrozen water column. Storage flux ($g\,m^{-2}\,yr^{-1}$) was calculated as the difference between total mass of dissolved gas in spring before ice breakup and the total mass of dissolved gas in summer.

2.5 CH_4 and CO_2 ebullition from sediments

We estimated CH_4 and CO_2 ebullition from sediments associated with discrete seeps following the lake-ice ebullition survey method of Walter Anthony et al. (2010). Seeps are defined as point-source locations of repeated bubbling and identified as A, B, C, and hotspot classes according to distinct patterns of bubbles trapped in lake ice (Appendix A2). To quantify seep ebullition, we removed snow from early winter lake ice to expose ebullition bubble clusters trapped in ice for seep classification, GPS mapping, flux measurements, and gas collection using submerged bubble traps. On foot, we surveyed 9355 individual seeps within 161 plots (30–300 m^2 per plot) positioned randomly within both littoral and profundal zones of lakes. In some lakes, ice was opened above the seeps for placement of submerged bubble traps. We retained semi-automated bubble traps placed over individual seeps year-round (Walter Anthony et al., 2010) to provide daily and seasonal ebullition flux data from sediments. Seep class-specific flux rates and bubble CH_4 and CO_2 concentrations measured on a subset of seeps were applied to all mapped seeps to estimate whole-lake ebullition rates, indexed by Julian day of the year (Appendix A2). These fluxes represent bubbling rates from sediments as measured at the lake surface, not necessarily direct ebullition to the atmosphere. The following two sections describe the fate of ebullition bubbles during the ice-cover and ice-free seasons.

2.6 Ice-bubble storage (IBS) flux

During the open-water (ice-free) summer season, ebullition bubbles reaching the lake surface release CH_4 directly to the atmosphere (direct ebullition). In winter, lake ice impedes direct ebullition emissions. Many ebullition bubbles reaching the top of the water column hit the underside of lake ice, come to rest, and exchange gases with the water column until the downward-growing ice encapsulates the bubbles. Since lake water is typically undersaturated in CH_4 with respect to the CH_4 concentration (40–90 %) of most ebullition bubbles (Sepulveda-Jauregui et al., 2012), CH_4 readily diffuses out of bubbles into the lake water column.

We collected 37 samples of ebullition bubbles trapped as pockets in lake ice from five Alaskan lakes, expanding upon the lake ice-bubble data set of Walter et al. (2008). Additionally, we opened the lake ice and placed bubble traps beneath ice, above seeps, to sample "fresh" ebullition bubbles at the lake surface before they are impeded by ice ($n = 2$–41 seeps per lake; total of 560 samples). This allowed us to compare concentrations of CH_4 in ice-trapped bubbles ($n = 2$–8 seeps per lake) to gas concentrations in "fresh" bubbles prior to ice entrapment.

Numerical modeling informed by detailed field studies of CH_4 diffusion from ice-trapped bubbles in one of our study lakes, Goldstream Lake (#18), revealed that 80 % of CH_4 in bubbles trapped by ice dissolves into the lake water column in winter (Greene et al., 2014). The remaining 20 % of CH_4 ebullition trapped by ice is released to the atmosphere, either from hotspot seep sites that open periodically throughout the winter or from A, B, and C seep sites as ice melts in spring (i.e., IBS emissions). With input of observed ice-growth rates on a subset of lakes in each of the three study regions and mean monthly atmospheric temperatures during 2003–2013 (US National Weather Service), we employed this model to calculate a first-order estimate of IBS in 34 of the 40 study lakes in which we had measurements of both seep ebullition and water-column dissolved CH_4 concentrations, which affect the CH_4 dissolution rate from bubbles. We linearly interpolated between measured surface CH_4 concentrations in the summer and spring to estimate water-column CH_4 concentrations during the ice-cover period. The decrease in the volume of ice-trapped bubbles in each lake, as calculated by this model, was used together with the decrease in their CH_4 concentration, calculated from our measurements of fresh vs. ice-trapped bubbles, to determine the IBS flux for each lake.

2.7 Direct ebullition in winter and summer

Since ice-bubble pockets above A-, B-, and C-type seeps open approximately 1 month prior to complete disappearance of lake ice in spring (K. M. Walter Anthony, unpublished data, 2014; Greene et al., 2014), we assume in our calculations that subsequent ebullition by seeps releases fresh bubbles directly to the atmosphere through open holes during this spring melt period. Particularly high bubbling rates from "hotspot" seeps maintain ice-free conditions above these point sources of bubbling, allowing for direct ebullition to the atmosphere when air temperature is higher than −15 °C (Zimov et al., 2001; Greene et al., 2014). In interior Alaska, the only region where hotspot seeps were observed, mean monthly temperatures from 2003 to 2013 indicated that on average, wintertime direct ebullition from hotspots occurs for several weeks post-freeze-up in October and in spring from February until ice melt in May. These shoulder seasons of bubble emissions through open holes in lake ice are consistent with our field observations. However, warm temperature anomalies or heavy snowfall events can also open hotspots at other times (on the scale of days) during winter (K. M. Walter Anthony, personal observation, 2014; Zimov et al., 2001; Greene et al., 2014), but these were not included in our calculations. In this study, ebullition from all seep classes during the final month of ice cover and from hotspots during fall and spring shoulder seasons when mean monthly atmospheric temperatures were higher than −15 °C (US National Weather Service) together comprised direct ebullition in winter.

Direct ebullition in summer was estimated as the product of average seep densities on each lake and the sum of daily ebullition measured in bubble traps placed on representative seeps of each class in a subset of lakes during the open-water summer period (Sect. 2.5).

2.8 Seasonal and mean annual emissions

We estimated mean annual emissions from lakes as the sum of various modes of emissions seasonally: (1) direct ebullition from all seeps and diffusion from the water column in summer (ice-free period); (2) winter (ice-cover period) direct ebullition emissions through ice-free hotspot seeps during shoulder seasons and from all open seeps during the final month of the spring ice-melt season; and (3) spring emissions as the sum of, first, the release of IBS (ebullition seep gases trapped by lake ice) before lake ice disappears and, second, the release of lake water column storage of dissolved gases, previously described by Michmerhuizen et al. (1996), Phelps et al. (1998), and Bastviken et al. (2004), when ice melts. We acknowledge that our calculations contain uncertainty associated with the assumption that single-day measurements of dissolved CO_2 and CH_4 in lakes represent the mean for calculating diffusion flux for the entire open-water period; however, these were the best available data at the time of this study, and a similar approach has been used in numerous other studies reviewed by Bastviken et al. (2011). Due to a paucity of field measurements on the Alaskan lakes, annual emissions estimates do not include background (non-seep) ebullition, which was found to be 25 % of annual emission in Siberian lakes (Walter et al., 2006).

Because lakes were classified according to three geographic zones based on climate and permafrost, the average

timing of ice cover was used to estimate the seasonal differences between CH_4 and CO_2 emissions for all lakes within each zone. Mean annual ice-on and ice-off dates from were compiled for years 2000–2012 for study lakes near Toolik Field Station in the northern region (1 October–18 June), our own observations of interior Alaska study lakes near Fairbanks from years 2008 to 2012 (8 October–9 May), and from Arp et al. (2013) and the National Park Service Inventory and Monitoring Program during years 2000–2013 for southern region lakes near Denali National Park (1 October–23 May) and south-central Alaska, south of the Alaska Range (15 November –7 May).

2.9 Physical and chemical limnology

We measured the physicochemical properties of lakes during winter and summer field campaigns at the same locations where dissolved gases were measured. Measurements of in situ water properties along vertical depth profiles in lakes included temperature, pH, oxidation reduction potential (ORP), and chlorophyll *a* (Chl *a*) obtained using a calibrated multiparametric probe Hydrolab DataSonde (Hach, Loveland, Colorado, USA). For a subset of lakes in each region, we used temperature data loggers (UA-001-08, Onset HOBO, Bourne, Massachusetts, USA) to record water temperature year-round in 5 min intervals at two depths (1 m water depth and lake bottom). Secchi disk depth (SecD) was measured with a 0.2 m Secchi disk. We collected water samples for ex situ analyses using a horizontal 2.2 L Van Dorn bottle (WILDCO, Yulee, Florida, USA). The concentrations of dissolved nitrate (NO_3^-), soluble reactive phosphorus (SRP), and sulfate (SO_4^{2-}) in lake water were measured with a high-performance liquid chromatograph equipped with an electrochemical detector (ED40 Dionex, Dionex, USA). We determined total organic carbon (TOC; used to approximate DOC following Wetzel , 2001, and Weyhenmeyer and Karlsson, 2009) and total nitrogen (TN) with a total carbon and nitrogen analyzer (Shimadzu TOC-Vcsh equipped with TNM1 module, Shimadzu, Japan).

Trophic state indexes (TSIs), calculated from Chl *a*, SecD, and SRP, were used to estimate the trophic states of the lakes (Carlson, 1977). Since total phosphorus (TP) is typically used in TSI calculations, our calculation is an approximation of trophic state. However, we do not expect the use of SRP instead of TP to have a large effect on our results, since Chl *a* is the primary index for trophic state classification (Carlson and Simpson, 1996). Furthermore, SRP is the more biologically reactive form of phosphorous in lake water lake, and has been shown to be a good predictor of trophic status (Stendick and Hall, 2003; Haberman and Haldna, 2014).

We classified some lakes as mixotrophic since our field and laboratory observations of brown water color (high DOC), low SecD, high nutrients, high epilimnetic Chl *a* concentrations, abundant macrophytes, and anoxic hypolimnion matched the definition of mixotrophic provided by Williamson et al. (1999). In these lakes, water had a dark-brown color resulting from high concentrations of DOC, presumably from humic substances and organic acids leached from litter and soils in their watersheds. Rather than recognizing two separate classes of high-DOC lakes (mixotrophy with high nutrient concentrations vs. dystrophy with low nutrient concentrations), Wetzel (2001) considered all high-DOC lakes as dystrophic. Wetzel (2001) explained that the productivity of most dystrophic lakes has classically been described as low; however, more detailed examinations indicated that chlorophyll concentration (phytoplankton biomass) was significantly higher in the more shallow photic zone of brown-water lakes than in clear lakes when expressed per volume of epilimnion. We did not quantify macrophyte biomass, but our qualitative observation of a higher abundance of submerged and emergent plants growing in the brown-water lakes is also consistent with Wetzel's description of littoral plants often contributing significantly to lake ecosystem metabolism in dystrophic (mixotrophic) lakes.

Surface sediment samples (1–5 cm depth) were collected in summer 2008 from a subset of lakes using a 6.6 cm diameter piston hammer corer at multiple locations within individual lakes. Samples were stored under refrigeration and then dried (105 °C) and acidified (5–15 mL 2N HCl), and subsequently the top 1 cm was analyzed for TOC and TN on a Costech ESC 4010 elemental analyzer (Alaska Stable Isotope Facility at the University of Alaska Water and Environmental Research Center). Additional surface lake sediment samples were collected in 2012 from a central lake location using the hammer corer. These sediments were analyzed for moisture content by weighing and drying to 105 °C. We determined organic matter content on a dry weight basis via loss on ignition at 550 °C (Dean, 1974).

2.10 Statistical analysis

Since data were not normally distributed and did not meet the assumption of homoscedasticity, we tested relationships between CH_4 and CO_2 emissions vs. geographic characteristics and limnological properties for the different lakes using the non-parametric two-tailed Mann–Whitney *U* test for comparison of two groups and Kruskal–Wallis one-way analysis of variance for comparison of several groups. We followed the Kruskal–Wallis analysis with the multiple-comparison *Z* value test; differences were significant when the *Z* value was > 1.96.

We used single linear regression analysis to quantify relationships between CH_4 and CO_2 emissions and geographic and limnological properties. For these analyses, data normalization was obtained using logarithm base 10 (log) transformation. Before and after data transformation, normality was assessed by the Shapiro–Wilk test. Regression models were accepted when the p value was < 0.01. Mean values from full vertical depth profiles of temperature, pH, and ORP, and

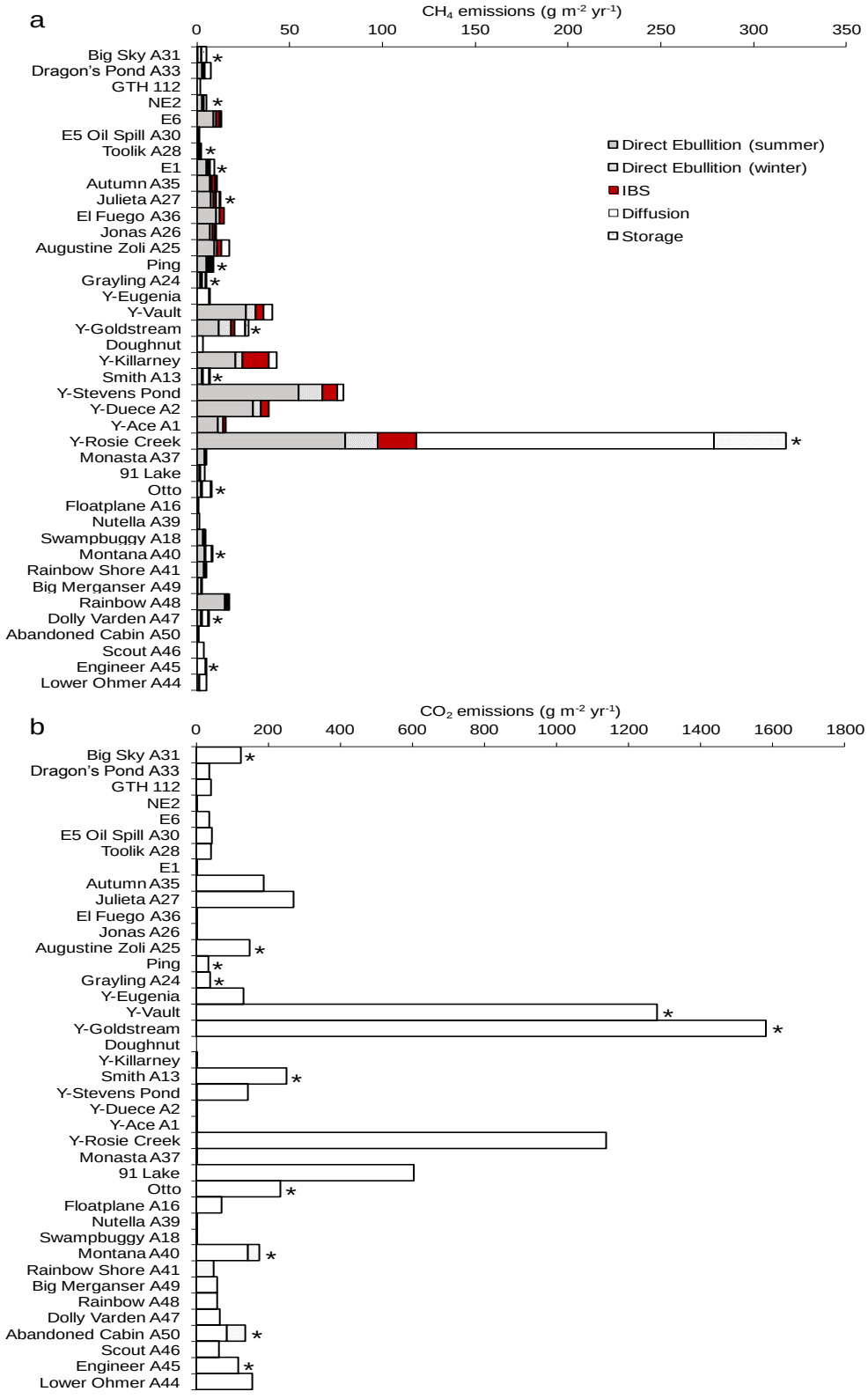

Figure 2. Total annual CH_4 **(a)** and CO_2 **(b)** emissions by mode from 40 lakes along a north–south latitudinal transect in Alaska. Yedoma lakes are indicated by "Y". Lakes for which all emission modes were measured are indicated by "∗" (see Table 2). Panels **(a)** and **(b)** follow the legend shown in **(a)**.

from epilimnion measurements for Chl *a* are shown in Table 1 and were used in these single linear regression analyses. We used the mean winter temperature measured with HOBO data loggers (1 m water depth and lake bottom) to fill data gaps in some northern lakes (Table 1).

Relationships between permafrost type, CH_4 ebullition, and lake area were evaluated graphically and by Spearman product-moment correlation coefficients (r_s). Relationships between lake-bottom water-dissolved CH_4, lake-bottom water-dissolved O_2, and ebullition were evaluated in the same manner.

Statistical analyses were performed with NCSS 2000 Statistical Analysis 193 System software (Number Cruncher Statistical Systems, USA). To fill data gaps, we added additional limnological, geographic, and ecological zone information from the literature to our own measurements (Table 1).

3 Results

3.1 Geographic and limnological patterns of CH_4 and CO_2 emissions

Total annual CH_4 and CO_2 emissions were highly variable, ranging 2 orders of magnitude among lakes (2.0 to > 300 g CH_4 and 34.2 to > 1500 g $CO_2\,m^{-2}\,yr^{-1}$; Table 2, Fig. 2). Among the geographic characteristics presented in Table 1 and CH_4 and CO_2 emissions presented in Table 2, we found that the type of permafrost soil (yedoma vs. non-yedoma) was the geographic characteristic most closely related to CH_4 and CO_2 emissions (Table 3). Total annual CH_4 emissions from yedoma lakes ($44.2 \pm 17.0\,g\,m^{-2}\,yr^{-1}$, mean $\pm$ SD, $n = 7$ lakes, excluding outlier lake #25) was significantly higher than from non-yedoma lakes ($8.0 \pm 4.1\,g\,m^{-2}\,yr^{-1}$, $n = 32$ lakes) (Table 2). Total annual CO_2 emissions appeared higher in yedoma ($784 \pm 757\,g\,m^{-2}\,yr^{-1}$, mean $\pm$ SD, $n = 8$ lakes, excluding outlier lake #25) than non-yedoma lakes ($137 \pm 129\,g\,m^{-2}\,yr^{-1}$, $n = 32$ lakes) (Table 2); however, due to high variability among lakes, the difference was not significant. Rosie Creek beaver pond (#25), an outlier lake with particularly high CH_4 and CO_2 emissions (317 g CH_4; 1138 g $CO_2\,m^{-2}\,yr^{-1}$; Fig. 2), was formed prior to our study by beaver activity in an active stream system that drains into the Tanana River. The pond was subsequently influenced by thermokarst expansion (K. M. Walter Anthony, personal observation) into yedoma-type deposits, which further enhanced carbon cycling in the fluvial system.

The relationship between CH_4 and CO_2 emissions and other geographic parameters followed the same pattern to the extent that they were related to characteristics of yedoma and non-yedoma permafrost soils (Table 3). For instance, yedoma is characterized by eolian deposits, which among the surface geologic deposit types was also most strongly related to CH_4 and CO_2 emissions. Among our study lakes, yedoma lakes occurred in the interior Alaska region (Fig. 1) and tended to have a mixotrophic state, parameters that were both related to CH_4 and CO_2 emissions. Since the particular yedoma lakes in our study were relatively small lakes ($\leq 0.1\,km^2$), lake area was a morphologic parameter closely related to CH_4 and CO_2 emissions.

Regressions models showed that physical and chemical limnological parameters (Table 1) explained 19–63 % of deviation in the different flux pathways of CH_4 emissions (Table 4). Total CH_4 emission was correlated with area, SecD, SRP, and TN (Table 4). We did not find any relationships between total CO_2 and the lakes' physicochemical properties, probably due to chemical equilibrium in water.

3.2 Modes of CH_4 and CO_2 emission

Total annual ebullition, consisting of direct ebullition in summer and winter as well as springtime release from IBS, was the dominant mode of CH_4 emission in lakes, comprising 86 % of total annual emissions from yedoma lakes and 65 % from non-yedoma lakes (Table 2). Summer direct ebullition was higher in yedoma-type lakes (26.2 ± 15.9 g $CH_4\,m^{-2}\,yr^{-1}$, $n = 6$ lakes, excluding lake #25) than non-yedoma lakes (4.0 ± 3.7 g $CH_4\,m^{-2}\,yr^{-1}$, $n = 28$ lakes). This contrast drove other significant relationships in the data set: since yedoma lakes were primarily located in the interior discontinuous permafrost zone, and they dominated the mixotrophic and northern boreal forest lakes category, we found that summer ebullition was higher in interior lakes than in northern and southern lakes; summer ebullition was higher in mixotrophic lakes than in lakes of other trophic states; and northern boreal forest lakes had higher summer direct ebullition than lakes from other ecozonal categories (Tables 2 and 3). Direct ebullition of CH_4 in winter and summer was correlated with lake area. Smaller lakes had higher direct ebullition (Table 4); since our yedoma study lakes were smaller than non-yedoma lakes, this factor is strongly influenced by permafrost type. The regression analysis with permafrost type categories separately (yedoma and non-yedoma lake type) creates scarce data in yedoma lakes ($n = 5$) to do this analysis. However, Spearman coefficients support this tendency, since it indicates a negative correlation with lake area among yedoma lakes (summer $r_s = -0.66$, winter $r_s = -0.71$) and in non-yedoma lakes (summer $r_s = -0.45$, winter $r_s = -0.63$).

Yedoma lakes were the only lakes in which we observed hotspot ebullition and seep densities of all seep classes were higher in yedoma lakes (mean $\pm$ SD: 2.12 ± 2.50 A seeps m^{-2}, 0.28 ± 0.19 B seeps m^{-2}, 0.06 ± 0.06 C seeps m^{-2}, 0.01 ± 0.01 hotspot seeps m^{-2}) compared to non-yedoma lakes (0.70 ± 0.68 A seeps m^{-2}, 0.05 ± 0.06 B seeps m^{-2}, 0.001 ± 0.003 C seeps m^{-2}, 0 hotspot seeps m^{-2}). It follows that direct ebullition during the winter ice-cover period was also much higher from yedoma lakes

Table 2. Total annual CH_4 and CO_2 emissions by mode from 40 lakes along a north–south latitudinal transect in Alaska. * indicates informal lake names. Eb. Sum. – direct ebullition emission to the atmosphere from seeps during the ice-free summer season; Eb. Win. – direct ebullition emission to the atmosphere from seeps during the ice-cover winter season; IBS – ice-bubble storage during spring ice melt; Stor. – storage emission following ice-out; Diff. – diffusive emission in summer; Total – total annual emissions. If there was ND (no determination) for one or more modes in a lake, then total annual emission for the lake is likely an underestimate. Average emissions are summarized at the bottom of the table, as is the percent of total annual emissions contributed by each mode as well as statistical results for differences in means among yedoma and non-yedoma lakes (Mann–Whitney test). Error terms represent standard deviation; *N* is the individual lake number and CF indicates impossible determination due to lake ice completely freezing to the lake bed in winter. CO_2 diffusive flux from lakes #17 and #18 were estimated from samples taken on multiple dates in June and July 2013 since no data were available in 2011–2012. Different letters[a,b] indicate a significant difference between yedoma and non-yedoma means.

N	Lake name	CH_4 ($g\,m^{-2}\,yr^{-1}$)					
		Eb. Sum.	Eb. Win.	IBS	Diff.	Stor.	Total
1	Big Sky* A31	0.2	0.0	0.1	2.0	2.7	5.0
2	Dragon's Pond* A33	3.0	0.6	0.6	3.2	ND	7.4
3	GTH 112	ND	ND	ND	2.0	0.0	2.0
4	NE2	2.8	0.5	0.5	1.3	0.0	5.1
5	E6	8.8	1.6	1.9	1.0	ND	13.3
6	E5 Oil Spill A30	0.4	0.1	0.1	0.9	ND	1.4
7	Toolik A28	0.6	0.1	0.1	0.9	0.2	2.0
8	E1	5.1	0.9	0.9	2.5	0.0	9.4
9	Autumn* A35	6.9	1.3	1.5	1.0	ND	10.7
10	Julieta* A27	7.5	1.3	1.6	1.9	0.0	12.3
11	El Fuego* A36	10.2	2.0	2.2	ND	ND	14.5
12	Jonas* A26	7.0	1.3	1.4	ND	0.7	10.4
13	Augustine Zoli* A25	9.3	1.7	2.3	4.5	ND	17.7
14	Ping*	5.1	1.0	1.0	1.0	0.9	9.0
15	Grayling A24	1.9	0.4	0.6	2.1	0.0	5.0
16	Eugenia*	ND	ND	ND	6.6	0.6	7.2
17	Vault*	26.6	4.9	4.5	4.8	ND	40.9
18	Goldstream*	13.4	6.7	2.3	6.0	1.9	30.3
19	Doughnut *	ND	ND	ND	3.1	ND	3.1
20	Killarney*	20.7	4.1	14.0	4.4	ND	43.3
21	Smith A13	2.7	0.3	0.4	3.2	0.2	6.7
22	Stevens Pond*	55.0	12.8	8.1	3.1	CF	79.0
23	Duece A2	30.1	4.2	4.6	ND	ND	38.9
24	Ace A1	11.4	2.7	1.5	ND	ND	15.6
25	Rosie Creek*	80.1	17.4	20.5	160.3	39.0	317.4
26	Monasta A37	4.1	0.3	0.7	ND	ND	5.1
27	91 Lake*	1.5	0.2	0.2	2.3	ND	4.2
28	Otto	2.1	0.2	0.3	4.9	0.6	8.1
29	Floatplane* A16	ND	ND	ND	1.1	ND	1.1
30	Nutella* A39	0.1	0.0	0.0	1.1	ND	1.3
31	Swampbuggy A18	3.2	0.3	0.4	0.8	ND	4.8
32	Montana A40	4.1	0.2	0.3	3.5	0.0	8.1
33	Rainbow Shore* A41	3.9	0.2	0.3	ND	0.9	5.4
34	Big Merganser A49	0.5	0.0	0.0	1.8	0.1	2.5
35	Rainbow A48	15.1	0.8	1.3	ND	0.0	17.2
36	Dolly Varden A47	2.4	0.1	0.2	3.2	0.9	6.8
37	Abandoned Cabin* A50	0.4	0.0	0.0	ND	ND	0.5
38	Scout A46	ND	ND	ND	3.6	0.0	3.6
39	Engineer A45	0.0	0.0	0.0	4.9	0.0	4.9
40	Lower Ohmer A44	1.4	0.1	0.1	3.6	ND	5.3
	Yedoma (mean ± SD)	26.2 ± 15.9^a	5.9 ± 3.6^a	5.8 ± 4.6^a	5.0 ± 1.4^a	1.2 ± 0.9^a	44.2 ± 17.0^a
	Percent	59 %	13 %	13 %	11 %	3 %	100 %
	Non-yedoma (mean ± SD)	4.0 ± 3.7^b	0.6 ± 0.6^b	0.7 ± 0.7^b	2.4 ± 1.3^b	0.4 ± 0.7^a	8.0 ± 4.1^b
	Percent	50 %	7 %	9 %	30 %	5 %	100 %
	All lakes (mean ± SD)					0.5 ± 0.7	

Table 2. Continued.

N	Lake name	CO_2 ($g\,m^{-2}\,yr^{-1}$)				
		Eb. Sum.	Eb. Win.	Diff.	Stor.	Total
1	Big Sky* A31	0.005	0.001	124	0	124.4
2	Dragon's Pond* A33	0.056	0.010	37	ND	37.1
3	GTH 112	ND	ND	42	ND	41.8
4	NE2	0.048	0.009	ND	ND	0.1
5	E6	0.153	0.028	36	ND	36.2
6	E5 Oil Spill A30	0.006	0.002	44	ND	44.3
7	Toolik A28	0.011	0.002	40	ND	40.5
8	E1	0.088	0.016	ND	ND	0.1
9	Autumn* A35	0.157	0.030	186	ND	186.5
10	Julieta* A27	0.128	0.023	270	ND	269.8
11	El Fuego* A36	0.181	0.036	ND	ND	0.2
12	Jonas* A26	0.122	0.023	ND	0	0.1
13	Augustine Zoli* A25	0.172	0.032	148	0	148.5
14	Ping*	0.097	0.018	34	0	34.2
15	Grayling A24	0.033	0.007	40	0	39.7
16	Eugenia*	ND	ND	131	ND	131.0
17	Vault*	0.445	0.099	1278	0	1279
18	Goldstream*	0.261	0.164	1582	0	1583
19	Doughnut *	ND	ND	ND	0	0.0
20	Killarney*	0.723	0.070	ND	0	0.8
21	Smith A13	0.052	0.006	251	0	250.9
22	Stevens Pond*	0.991	0.292	144	CF	144.9
23	Duece A2	0.477	0.087	ND	0	0.6
24	Ace A1	0.196	0.059	ND	0	0.3
25	Rosie Creek*	1.462	0.404	1136	ND	1138
26	Monasta A37	0.076	0.005	ND	ND	0.1
27	91 Lake*	0.029	0.003	604	ND	604.2
28	Otto	0.040	0.004	234	0	233.9
29	Floatplane* A16	ND	ND	69	ND	69.5
30	Nutella* A39	0.002	0.000	ND	ND	0.0
31	Swampbuggy A18	0.056	0.006	ND	ND	0.1
32	Montana A40	0.076	0.004	143	33	176.4
33	Rainbow Shore* A41	0.075	0.004	ND	48	47.6
34	Big Merganser A49	0.010	0.001	59	ND	58.9
35	Rainbow A48	0.289	0.016	59	ND	59.4
36	Dolly Varden A47	0.047	0.003	65	ND	64.7
37	Abandoned Cabin* A50	0.008	0.000	85	52	137.5
38	Scout A46	ND	ND	64	0	63.9
39	Engineer A45	0.000	0.000	118	0	117.8
40	Lower Ohmer A44	0.027	0.001	157	ND	156.6
	Yedoma (mean ± SD)	0.5 ± 0.3^{a}	0.13 ± 0.09^{a}	784 ± 757^{a}	0^{a}	784 ± 757^{a}
	Percent	0.07 %	0.02 %	100 %	0 %	100 %
	Non-yedoma (mean ± SD)	0.07 ± 0.07^{b}	0.01 ± 0.01^{b}	127 ± 127^{b}	10 ± 20^{a}	137 ± 129^{a}
	Percent	0.05 %	0.01 %	92 %	7 %	100 %
	All lakes (mean ± SD)				7 ± 17	159 ± 322

Table 3. The Mann–Whitney and Kruskal–Wallis test results of the limnological and geographic characteristics of lakes using CH_4 or CO_2 emission mode as the factor. "≠" indicates a significant difference between limnological property or geographic characteristic vs. flux; "=" indicates no significant difference at Z value < 1.96. IBS – ice-bubble storage; Latitude: I – interior, N – northern, and S – southern according to Sect. 2.1; permafrost soil type (Y/NY – yedoma/non-yedoma); trophic state index (TSI), ecozonal categories (EC), and deposit type (DN) according to descriptions in Table 1; maximum depth known (MD) and area (A). In the MD analysis we considered two categories: shallow lakes ≤ 2.5 m and deeper lakes > 2.5 m. In the A analysis we considered two categories: small lakes ≤ 0.1 km^2 and large lakes > 0.1 km^2.

Emission mode	Latitude	Y/NY	TSI	EC	DN	MD	A
CH_4							
Direct ebullition (summer)	I ≠ N-S	≠	O ≠ Mx-UO	NBF ≠ ArT-SBF	=	=	≠
Direct ebullition (winter)	S ≠ I-N	≠	O ≠ Mx-UO	SBF ≠ FoT-NBF	E ≠ GMD-GL	=	≠
IBS	S ≠ I-N	≠	O ≠ Mx-UO	SBF ≠ FoT-NBF	E ≠ GL	=	≠
Diffusion	I ≠ N	≠	D ≠ O-UO	ArT ≠ NBF-SBF	=	=	=
Storage	=	=	=	=	=	=	=
Total	I ≠ S	≠	O ≠ Mx-UO	=	GL ≠ E-GMD	=	≠
CO_2							
Direct ebullition (summer)	I ≠ N-S	≠	O ≠ Mx-UO	NBF ≠ ArT-SBF	E ≠ GMD-GL	=	≠
Direct ebullition (winter)	S ≠ I-N	≠	O ≠ Mx-UO	SBF ≠ FoT-NBF	E ≠ GMD-GL	=	≠
Diffusion	I ≠ N	≠	=	NBF ≠ ArT-FoT-SBF	=	=	≠
Storage	=	=	=	=	=	=	=
Total	=	=	=	=	=	=	=

(5.9 ± 3.6 g CH_4 m^{-2} yr^{-1}, $n = 6$ lakes; excluding lake #25) than non-yedoma lakes (0.6 ± 0.6 g CH_4 m^{-2} yr^{-1}, $n = 28$ lakes) (Table 2). In contrast, ebullition was not an important mode of CO_2 emission from any lakes. Total ebullition, including summer and winter direct ebullition, contributed 0.1 % of the total annual CO_2 emissions among all lakes (Table 2).

A comparison of CH_4 composition in fresh ebullition bubbles vs. bubbles trapped by lake ice revealed that the CH_4 concentration in ebullition bubbles trapped by ice was 33 ± 12 % (mean ± SD, $n = 6$ lakes) lower than in ebullition bubbles escaping to the atmosphere at the lake surface unimpeded by ice (Fig. 3; Mann–Whitney U test, $Z > 1.96$, $p < 0.05$).

The IBS model, which accounts for decreases in the volume and CH_4 concentration of ice-trapped bubbles as their CH_4 dissolves into the water column (Greene et al., 2014), revealed that IBS was on average 13 % of total annual CH_4 emissions from yedoma lakes (5.8 ± 4.6 g m^{-2} yr^{-1}, $n = 6$) and 9 % for non-yedoma lakes (0.7 ± 0.7 g m^{-2} yr^{-1}, $n = 28$) (Table 2, Fig. 2). The CH_4 IBS flux from lakes was negatively correlated with area and SecD (Table 4). Given the minor role of CO_2 direct ebullition in the annual emission budget (< 0.1 %), and the even smaller role of springtime IBS, we considered IBS an insignificant mode of CO_2 emission.

Storage emissions were highly variable among all lakes (0.5 ± 0.7 g CH_4 m^{-2} yr^{-1}, $n = 20$ lakes; 7 ± 17 g CO_2 m^{-2} yr^{-1}, $n = 18$ lakes; excluding lake #25). We did not find a significant difference in storage flux between yedoma vs. non-yedoma lakes. As with all modes of emission, lake #25 had the highest storage CH_4 flux (39.0 g m^{-2} yr^{-1}). We did not find a correlation between CH_4 storage flux and limnological parameters ($p < 0.01$). Since we were unable to normalize the CO_2 storage flux data, it was not possible to assess potential correlations between this mode of emission and limnological parameters. In the comparison of emission modes, storage flux contributed 3 and 0 % of total annual CH_4 and CO_2 emissions, respectively, from yedoma lakes and 5 and 7 % of total annual CH_4 and CO_2 emissions, respectively, from non-yedoma lakes (Table 2).

CH_4 diffusion emissions were statistically different between yedoma (5.0 ± 1.4 g CH_4 m^{-2} yr^{-1}, $n = 5$; excluding lake #25) and non-yedoma lakes (2.4 ± 1.3 g CH_4 m^{-2} yr^{-1}, $n = 26$). Rosie Creek beaver pond (#25) had the highest diffusive flux (160.3 g CH_4 m^{-2} yr^{-1}). Diffusion comprised 11 and 30 % of total annual CH_4 emissions from yedoma and non-yedoma lakes, respectively. We found a significant positive correlation between CH_4 diffusive flux and SRP (Table 4). In contrast, diffusion was the dominant CO_2 mode of emission among all of our study lakes. Diffusion constituted 100 and 92 % of CO_2 emissions from yedoma and non-yedoma lakes, respectively. Diffusion from yedoma lakes (784 ± 757 g CO_2 m^{-2} yr^{-1}, $n = 4$ lakes) was significantly higher than diffusion from non-yedoma lakes (127 ± 127 g CO_2 m^{-2} yr^{-1}, $n = 23$ lakes). It was not possible to normalize CO_2 diffusion data, so we were unable to determine potential correlations between this mode of emission and limnological parameters.

Table 4. Single regression equations for emission modes based on data from Table 1.

Flux/characteristic	Regression equation	n	Adjusted r^2	F	p
CH_4					
Direct ebullition (summer)	$\text{Log(ES-CH}_4) = -0.50\text{Log(area)}$	32	0.30	14.4919	0.0006
Direct ebullition (winter)	$\text{Log(EW-CH}_4) = -0.93 - 0.68\text{Log(area)}$	28	0.60	43.6036	0.0000
	$\text{Log(EW-CH}_4) = 0.10 - 1.12\text{Log(SecD)}$	28	0.23	9.3352	0.0050
	$\text{Log(EW-CH}_4) = -2.63 + 0.81\text{Log(TN)}$	24	0.32	12.4092	0.0018
IBS	$\text{Log(IBS-CH}_4) = -0.83 - 0.64\text{Log(area)}$	29	0.58	50.705	0.0001
	$\text{Log(IBS-CH}_4) = 0.10 - 1.00\text{Log(SecD)}$	29	0.19	7.9309	0.0088
Diffusion	$\text{Log(DF-CH}_4) = 0.55\text{Log(SRP)}$	24	0.40	16.7767	0.0004
Total	$\text{Log(Tot-CH}_4) = 0.43 - 0.37\text{Log(area)}$	38	0.27	15.0877	0.0004
	$\text{Log(Tot-CH}_4) = 1.01 - 0.77\text{(SecD)}$	38	0.21	11.1414	0.0019
	$\text{Log(Tot-CH}_4) = 0.42 + 0.55\text{Log(SRP)}$	30	0.22	9.4969	0.0045
	$\text{Log(Tot-CH}_4) = 0.98 - 0.61\text{Log(TN)}$	32	0.29	13.7928	0.0008
CO_2					
Direct ebullition (summer)	$\text{Log(ES-CO}_2) = -1.72 - 0.50\text{Log(area)}$	32	0.30	14.6253	0.0006
Direct ebullition (winter)	$\text{Log(EW-CO}_2) = -2.78 - 0.76\text{Log(area)}$	30	0.63	52.0960	0.0000
	$\text{Log(EW-CO}_2) = -1.83 - 0.76\text{Log(TN)}$	26	0.24	9.0882	0.0058

Table 5. Mann–Whitney and Kruskal–Wallis test results for the relationships between limnological and geographic characteristics of lakes vs. dissolved gas concentrations (CH_4 or O_2) during winter and summer. "$\neq$" indicates a significant difference between a geographic characteristic and flux when $Z > 1.96$; "=" indicates no significant difference. Latitude: I – interior, N – northern, and S – southern according to Sect. 2.1; permafrost soil type (Y/NY – yedoma/non-yedoma); trophic state index (TSI), ecozonal categories (EC), and deposit type (DN) according to descriptions in Table 1; maximum depth known (MD) and area (A). In the MD analysis we considered two categories: shallow lakes ≤ 2.5 m and deeper lakes > 2.5 m. In the A analysis we considered two categories: small lakes $\leq 0.1\,\text{km}^2$ and large lakes $> 0.1\,\text{km}^2$.

Dissolved gas (season)	Latitude	Y/NY	TS	EC	DN	MD	A
CH_4 (winter)	I $\neq$ S	$\neq$	Mx $\neq$ O	=	E $\neq$ GL, GMD	$\neq$	$\neq$
CH_4 (summer)	I $\neq$ N, S	$\neq$	Mx $\neq$ O, UO	NBF $\neq$ ArT, SBF, FoT	E $\neq$ GMD	=	$\neq$
O_2 (winter)	I $\neq$ S	$\neq$	Mx $\neq$ O	=	E $\neq$ GL, GMD	=	$\neq$
O_2 (summer)	I $\neq$ N, S	$\neq$	Mx $\neq$ O, UO	NBF $\neq$ ArT, SBF, FoT	E $\neq$ GL, GMD	=	$\neq$

3.3 Seasonal emissions

Figure 4 illustrates the contribution of different gas emissions pathways to annual emissions by season. Approximately three-quarters of annual CH_4 emissions were released from lakes during the open-water summer season: 71 and 79 % of total annual CH_4 emissions in yedoma lakes and non-yedoma lakes, respectively, were the sum of summer direct ebullition and diffusion. Spring and winter CH_4 emissions were also important. From yedoma lakes, first 13 % of total annual emissions occurred via IBS in spring, when the ice started to degrade; subsequently, water column storage release of dissolved gases was 3 % of total annual emissions. From non-yedoma lakes, total springtime emissions were 14 % of annual, consisting first of IBS (9 %) followed by storage (5 %). Wintertime emissions via direct ebullition from ice-free holes above seeps were 13 % of total annual emissions from yedoma lakes and 7 % from non-yedoma lakes. It is of interest to note that accounting for IBS, a newly recognized mode of emission, increased the estimate of springtime CH_4 emissions based on the more commonly reported storage emission by 320 %.

Seasonally, ~ 100 and 92 % of total annual CO_2 emissions from yedoma and non-yedoma lakes, respectively, occurred in summer by diffusion from the open-water surface. The remaining 8 % of annual emissions in non-yedoma lakes occurred in spring from water column storage flux (7 %) and winter direct ebullition (< 1 %) (Table 2 and Fig. 2).

3.4 Physical and chemical patterns

The difference between yedoma and non-yedoma lakes was observed in several physical and chemical parameters (Ta-

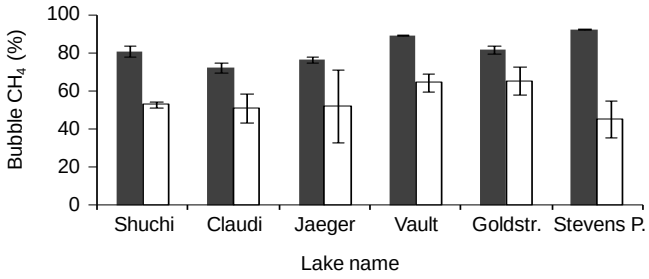

Figure 3. Average CH_4 concentrations in ebullition bubbles collected at the lake surface before interaction with lake ice ("fresh bubbles", grey bars) and in ebullition bubbles trapped by the lake ice (white bars). Error bars represent standard error for $n = 2$ to 41 seeps per lake. Among lakes, CH_4 concentrations in ice-trapped bubbles were 33 ± 12 % lower than in fresh bubbles (Mann–Whitney U test, $Z > 1.96$, $p < 0.05$).

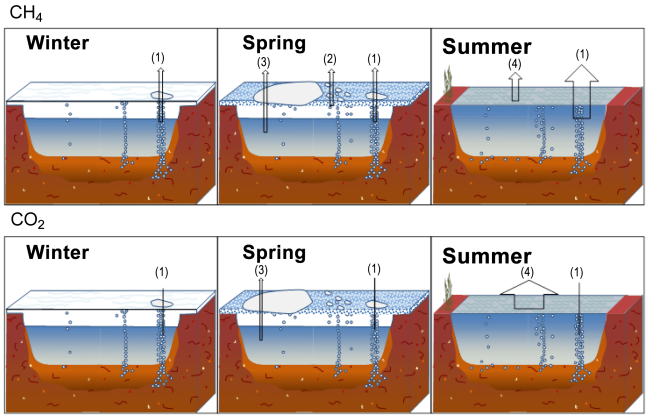

Figure 4. Illustration of CH_4 and CO_2 emissions pathways during different seasons in Alaskan lakes. The thickness of arrows indicates the relative magnitude of contribution from each pathway according to Table 2: (1) direct ebullition through ice-free hotspot seeps in winter and from all seep classes during the last month of ice cover in spring and in summer, (2) ice-bubble storage (IBS) emission during spring ice melt, (3) storage emission of dissolved gases accumulated under lake ice when ice melts in spring, and (4) diffusion emission from open water in summer.

bles 1, 3, and 5). Southern lakes (non-yedoma lakes) are deeper and larger than interior lakes (mostly yedoma lakes), while northern lakes (non-yedoma lakes) were not statistically different from lakes in the other regions.

Deep lakes (> 20 m), moderately deep lakes (usually > 6 m) with adequate wind protection from topography and/or vegetation, and all yedoma lakes, owing to their small surface area to volume ratios and high TOC concentrations, were thermally stratified in summer. Exceptions were two yedoma-type lakes with creeks flowing through them (Killarney Lake #20 and Rosie Creek beaver pond #25) and a small, shallow, yedoma thermokarst pond (Stevens Pond #22, 1.1 m) that was semi-stratified. In contrast, shallow, non-yedoma lakes (usually < 3 m) and non-yedoma lakes located in mountain regions with large surface area to volume ratios and high wind conditions were well mixed.

In winter, most lakes showed inverse stratification. We found that winter bottom temperature was significantly different between northern lakes (1.3 ± 1.5 °C) and southern lakes (2.6 ± 1.1 °C), but none of these were significantly different from lake bottom temperature in interior Alaska (1.4 ± 1.0 °C), which is mainly due to the contrasting climatic conditions and the relatively shallow depths of northern lakes compared to southern lakes.

In most lakes, if there was a dissolved O_2 (DO) gradient, then DO was highest near the lake surface and decreased with depth in winter and summer. Three exceptions were El Fuego Lake (#11), 91 Lake (#27), and Dolly Varden Lake (#36), where we observed an increase in DO with depth in summer, likely due to benthic photosynthesis in the shallow lakes (#11 and #27) and a deep chlorophyll maximum (DCM) in the deep lake (#36). In #36 we observed Chl *a* concentrations near the surface of ~ 3.7 µg L^{-1}; Chl *a* concentrations increased with depth to a maximum (23.0 µg L^{-1}) just below 20 m. DCM is a common trend in deep, clear-water lakes with low trophic state (Gervais et al., 1997; Camacho, 2006). Among yedoma lakes, lake-bottom dissolved oxygen (DO) concentrations were < 0.1 mg L^{-1} in both winter and summer. In contrast, 81 % of the 32 non-yedoma lakes had well-oxygenated lake bottoms in summer; the lake-bottom water DO concentration in the other 19 % of lakes was < 0.1 mg L^{-1}. In winter, we observed the reverse pattern among non-yedoma lakes: 76 % of 17 non-yedoma lakes measured had lake-bottom DO < 0.1 mg L^{-1}, while 24 % of non-yedoma lakes, all of which were southern lakes, had well-oxygenated lake bottoms in winter. All temperature and DO profiles measured on the study lakes are shown in Supplement Fig. S1.

DO concentrations were inversely related to dissolved CH_4 concentrations in the lake bottom water during winter and summer (Fig. 5). This relationship suggests a strong influence by microbial processes that consume O_2, consequently reducing aerobic oxidation of dissolved CH_4, particularly in the organic-rich, yedoma lakes of interior Alaska (Table 5 and Sect. 4.3). Additionally, we found significant statistical relationships between lake area and dissolved gas concentrations (CH_4 and O_2) among our yedoma (small lakes) and non-yedoma study lakes (generally larger lakes) (Table 5).

Five additional limnological parameters also showed significant differences between yedoma and non-yedoma lakes (Table 1). The TOC, SRP, TN, Chl *a*, and SecD indicated higher nutrient availability and higher primary production in the mixotrophic, yedoma lakes and/or their watersheds (Table 1). ORP values were significantly different between winter and summer in all lakes (Table 1), but were more than 2.5 and 1.5 times lower in yedoma lakes compared to

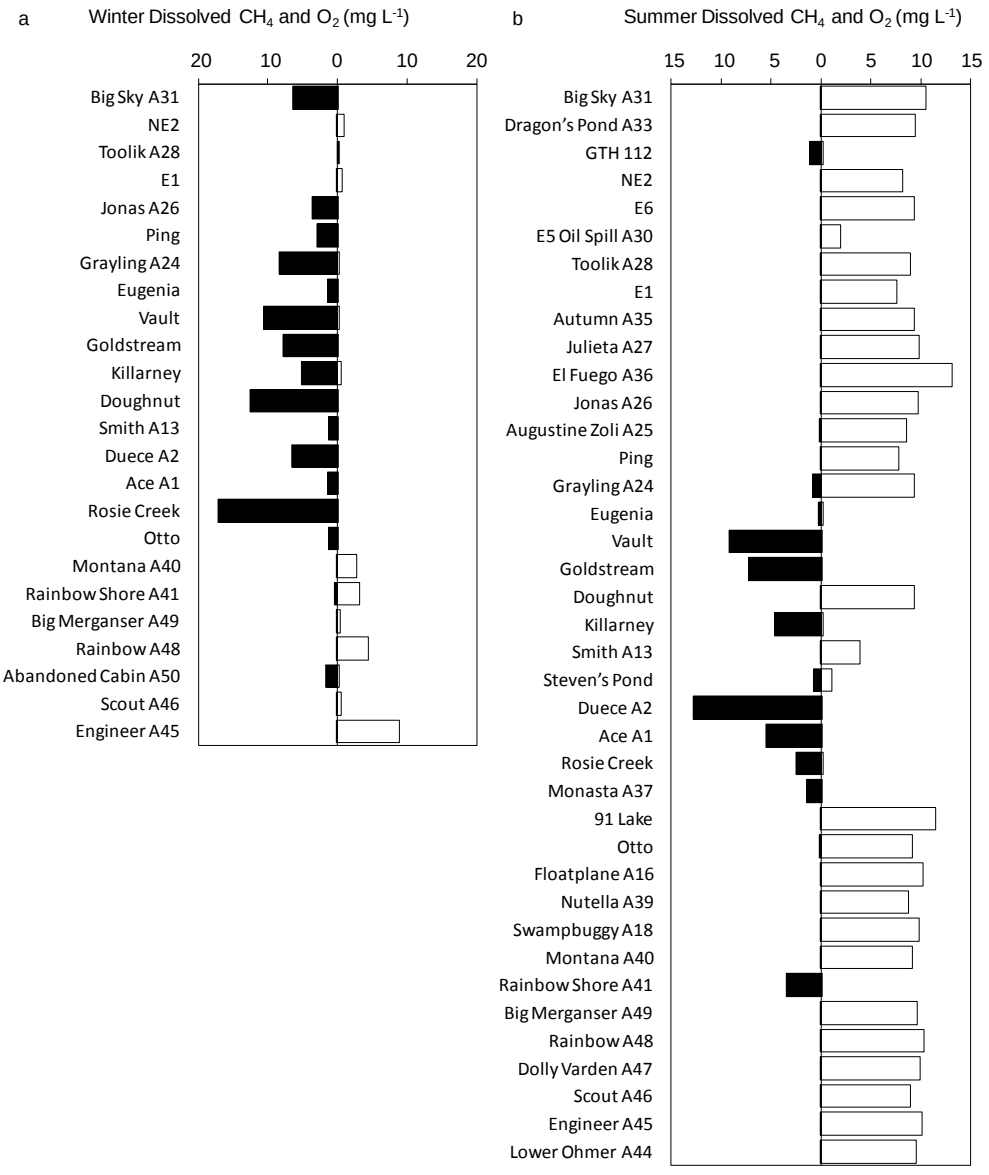

Figure 5. Average dissolved CH_4 (black bars) and O_2 (white bars) concentrations in lake bottom water during winter **(a)** and summer **(b)**. Yedoma lakes are indicated by "Y". In winter, a Spearman coefficient of $r_s = 0.58$ indicates a moderate positive correlation between dissolved CH_4 and O_2; in summer $r_s = 0.70$ indicates a strong positive correlation.

non-yedoma lakes in winter and summer, respectively, indicating greater reducing conditions in yedoma-lake water columns. Temperature and pH were significantly different between summer and winter in non-yedoma lakes, while only temperature differed seasonally in yedoma lakes. Altogether, these findings of higher primary production and lower ORP are consistent with the observations of high CH_4 and low O_2 concentrations in yedoma lakes compared to non-yedoma lakes (Fig. 5).

4 Discussion

4.1 Emission modes

The relative magnitude of different emission modes in this study followed the same general pattern observed previously (Casper et al., 2000; Bastviken et al., 2004; Abril et al., 2005; Repo et al., 2007), with ebullition dominating lake CH_4 emissions and diffusion dominating CO_2 emissions. Most studies of ebullition are conducted by distributing bubble traps in lakes without prior knowledge of discrete seep locations. Since seep locations are identified in winter as vertical stacks of bubbles in lake ice that represent repeated ebul-

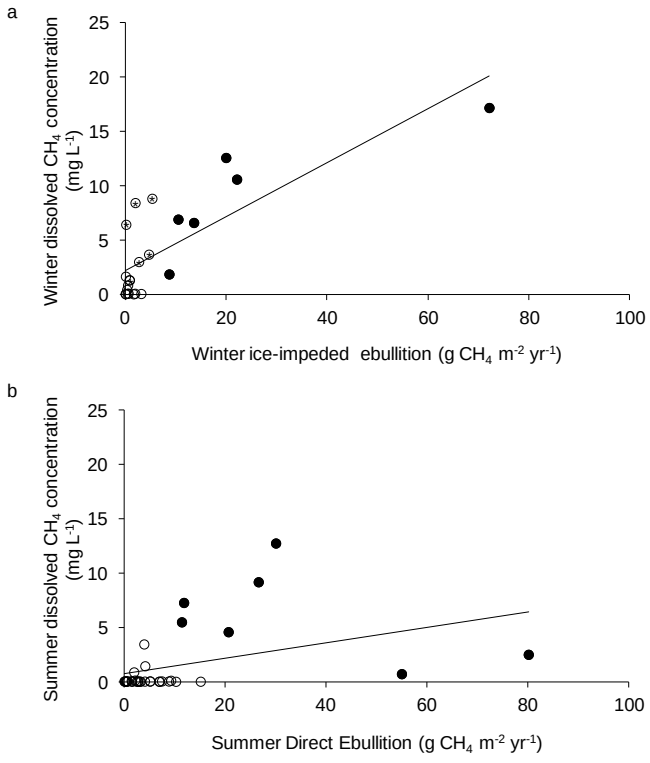

Figure 6. Dissolved CH_4 concentrations measured in lake bottom water vs. winter ice-impeded ebullition in winter **(a)** and direct ebullition in summer **(b)**. The Spearman coefficients, $r_s = 0.72$ and $r_s = 0.42$, indicate a strong positive correlation and a weak positive correlation in winter and summer, respectively. All lakes were considered a single population; however, yedoma lakes (closed circles) had higher concentrations of lake-bottom dissolved CH_4 (mean $\pm$SD: 9.3 ± 5.4 winter, $6.7 \pm 4.1\,\mathrm{mg\,L^{-1}}$ summer) and a higher density of ebullition seeps (Sect. 3.2) than non-yedoma lakes (open circles; 2.1 ± 3.0 winter, $0.3 \pm 0.7\,\mathrm{mg\,L^{-1}}$ summer). We observed relatively high concentrations of dissolved CH_4 in some non-yedoma lakes in winter due to dissolved gas exclusion during ice formation in shallow lakes that nearly froze to the lake bed, indicated by "$*$". Excluding lakes that nearly froze to the lake bed, the mean dissolved CH_4 in the remaining non-yedoma lakes was $0.3 \pm 0.5\,\mathrm{mg\,L^{-1}}$ in winter.

lition from discrete point sources, surveys of lake-ice bubbles reveal the locations and densities of ebullition seeps on lakes. Surveys also show the relative proportion of (ebullition) bubble-free black ice, which in nearly all ice-covered lakes dominates on an area basis. Walter et al. (2006) identified non-point-source bubbling from the seep-free fraction of the lake as "background ebullition". Background ebullition is thought to originate primarily from methanogenesis in surface lake sediments in summer; in contrast, ebullition seeps consist of bubble tubes that allow CH_4 produced at depth in sediments to migrate efficiently as bubbles to the sediment surface in summer and winter by the repeated release from point-source locations. Bubble traps placed in seep and non-seep locations and monitored year-round in two Siberian lakes showed that seep ebullition dominated total annual CH_4 emissions. Background ebullition was high in summer, nearly absent in winter, and altogether comprised $\sim 25\,\%$ of total annual CH_4 emissions in the Siberian lakes. Preliminary results from bubble traps placed in some of our Alaskan study lakes in locations where no seep ebullition bubbles were observed in winter also showed high summertime bubbling (K. M. Walter Anthony, unpublished data, 2014). This suggests that background ebullition occurs in Alaska too. Since our estimate of lake ebullition in the Alaskan lakes is based solely on discrete seeps and does not include non-seep background ebullition, we consider that our estimate of total lake ebullition is below the total actual ebullition flux. Given that methanogenesis is highly temperature dependent (Dunfield et al., 1993; Schulz et al., 1997; Duc et al., 2010; Marotta et al. 2014; Yvon-Durocher et al. 2014) and that surface lake sediments heat up in summer, accounting for background ebullition would likely increase the total ebullition emissions from all of the Alaskan study lakes.

The ice-bubble storage (IBS) mode of emission described here is a newly recognized CH_4 ebullition flux component in lakes (Greene et al., 2014) that has not previously been included in regional studies. Given the coarse temporal resolution of temperature and dissolved gas data used as input to the IBS model, we acknowledge that our estimate of IBS is a first-order approximation. However, strong agreement in the relative importance of IBS in the annual CH_4 budget of Goldstream Lake (#18) in this study using coarse-resolution data (IBS 6 % of total annual CH_4 emission) vs. the estimate from Greene et al. (2014) using highly detailed field data allowing detailed modeling (IBS was 6 and 9 % of total annual emissions in two different years) suggests that our first-order approximations of IBS may be valid. Since IBS was an important mode of CH_4 emissions among our study lakes (13 and 9 % of total annual emissions in yedoma and non-yedoma lakes, respectively), it is likely that past estimates of the magnitude and seasonality of CH_4 emissions from lakes with ebullition seeps were incomplete. Greene et al. (2014) found that a large fraction ($\sim 80\,\%$) of CH_4 diffused from ebullition bubbles trapped under lake ice into the lake water in Goldstream Lake. Coarser-resolution modeling of the IBS process for our study lakes also suggested that approximately 80 % of CH_4 dissolved out of ice-trapped bubbles. The mean and standard deviation of the CH_4 fraction dissolving out of ice-trapped bubbles was $83 \pm 0.9\,\%$ for 34 lakes (range 65–89 % for 33 lakes, excluding Killarney Lake with anomalously low CH_4 content in bubbles freshly released from sediments). Detailed measurements and modeling in Goldstream Lake showed that about half of this redissolved CH_4 was ultimately oxidized (Greene et al., 2014). Due to a paucity of field data, we did not model CH_4 oxidation; however, given the observed CH_4 oxidation potentials in our study lakes through incubation studies (Martinez-Cruz et al., 2015), it is likely that some fraction of the redissolved ebullition bub-

bles is oxidized. The unoxidized fraction of dissolved CH_4 is subject to release to the atmosphere via water column convection and diffusion as storage emissions in spring when ice more completely disintegrates and as diffusion during summer (Greene et al., 2014). Thus the storage and diffusion modes of emission may involve not only dissolved CH_4 that diffused out of lake sediments but also dissolved CH_4 that first originated as ebullition bubbles prior to ice entrapment. Since ebullition seeps were important components of whole-lake CH_4 emissions in all of our study lakes, as well as in tens of other lakes previously reported in Alaska (Walter Anthony et al., 2012) and Siberia (Walter et al., 2006; Walter Anthony et al., 2010), IBS should be studied and accounted for in global lake CH_4 emission budgets.

Lake CH_4 storage emission estimates for our Alaska study lakes (0.5 ± 0.7 g CH_4 m^{-2} yr^{-1}; Table 2), which comprised ~ 4 % of total annual emissions, were highly variable and on the same order of magnitude as the mean estimate for other northern lakes reported by Bastviken et al. (2004) (2.4 g CH_4 m^{-2} yr^{-1}) and Bastviken et al. (2011) (0.8 g CH_4 m^{-2} yr^{-1}; pan-Arctic). Storage emissions from global lakes ranged from < 0.1 to 37 g CH_4 m^{-2} yr^{-1}, comprising 0.5 to 81 % of the total annual emissions (Bastviken et al., 2011). This also suggests high variability in this emission mode among global lakes. The large relative error for storage flux measured among our Alaska study lakes (140 %; mean $\pm$SD, 0.5 ± 0.7 g CH_4 m^{-2} yr^{-1}) confirms that there is large variability associated with this mode of emission; however, CH_4 storage emissions in our Alaska study lakes were < 2.7 g CH_4 m^{-2} yr^{-1}, except in Rosie Creek beaver pond (#25, 39 g CH_4 m^{-2} yr^{-1}). The small sample size ($n = 2$ yedoma lakes) might lead to potential bias in the storage emissions for yedoma vs. non-yedoma lakes. Further analyses are required to address the differences in storage emissions between these lake types. Additionally, full or partial turnover of the lake water column in fall can release additional stored CH_4 (Bastviken et al., 2004; Bellido et al., 2009). We acknowledge that our storage values for CH_4 and CO_2 are gross estimations since we estimated only spring storage emission and did not take into account potential additional emissions associated with fall turnover or the impacts of lake morphology. Low spatiotemporal resolution sampling to calculate storage emissions also introduces imprecision in our estimates. A better method would involve continuous measurements of dissolved CH_4 and CO_2, temperature, and pH in lake water column at multiple locations in the lake throughout the full ice-melt period.

4.2 Geographic patterns of lake CH_4 and CO_2 emissions in Alaska

Previous regional analyses of northern lake emissions found a relationship between CH_4 emissions from lakes and latitude that was explained by temperature (Marotta et al., 2014; Rasilo et al., 2015; Yvon-Durocher et al., 2014). Primary production in warmer climates may supply more organic substrate for methanogenesis (Duc et al., 2010; Ortiz-Llorente and Alvarez-Cobelas, 2012; Marotta et al., 2014), and methanogenesis is physiologically sensitive to temperature (Schulz et al., 1997; Yvon-Durocher et al., 2014). However, the lakes in these studies were not permafrost-affected. In our north–south Alaska transect we did not find a relationship between any pathway of lake CH_4 emissions and latitude or temperature. We attribute this finding to the presence and geographic diversity of permafrost types (yedoma vs. non-yedoma) (Jorgenson et al., 2008; Kanevskiy et al., 2011), which is more a function of periglacial history and topography in Alaska than it is of latitude or recent climate. While methanogenesis in surface sediments of lakes globally is fueled by contemporary autochthonous primary production and allochthonous organic matter supply (processes typically controlled by latitude and climate in undisturbed systems), thermokarst-influenced lakes have an additional, deeper source of organic matter that fuels methanogenesis: thawing permafrost in the thaw bulbs beneath lakes and along thermally eroding shorelines. Organic matter supplied by thawing permafrost, particularly in lakes formed in thick, organic-rich, yedoma-type deposits, can supply more substrate to methanogenesis than the more contemporary organic carbon substrates supplied to surface lake sediments (Kessler et al., 2012).

The interior Alaska yedoma lakes, which had the highest CH_4 and CO_2 emissions, are largely thermokarst lakes formed by thaw of organic-rich yedoma permafrost. Radiocarbon ages (18–33 kyr BP) and δMx-depleted values of CH_4 in ebullition bubbles collected from the interior Alaskan thermokarst lakes suggested that thaw of late Pleistocene yedoma organic matter fuels methanogenesis in these lakes (Walter et al., 2008; Brosius et al., 2012). The 6-fold difference in CH_4 emissions between yedoma lakes and non-yedoma lakes throughout the rest of Alaska is likely explained by the variability in the availability of recently thawed permafrost organic matter, which provides a larger additional substrate for methanogenesis in the yedoma lakes owing to the thickness (usually tens of meters) of organic-rich yedoma deposits (Kanevskiy et al., 2011; Walter Anthony et al., 2012).

Previous research using stable isotopes and radiocarbon dating of CH_4 in ebullition bubbles in yedoma lakes demonstrated that stronger ebullition seeps originate from greater depths beneath the sediment interface and are characterized by older ^{14}C ages and more depleted δD values associated with thaw of Pleistocene-aged yedoma permafrost (Walter et al., 2008). The disproportionately large contribution of strong hotspot ebullition seeps to emissions from yedoma lakes (mean $\pm$ SD: 17 ± 12 % of total annual emissions) in this study suggests microbial production of CH_4 at greater depths in sediments beneath yedoma lakes. In contrast, the absence of hotspot ebullition seeps in non-yedoma lakes, which we observed to also have dense sediments, suggests

that CH_4 formation by microbial decomposition of organic matter is more restricted to shallower sediment depths in the non-yedoma lakes. This is consistent with maps of permafrost soil organic carbon distributions, whereby the organic horizons of non-yedoma permafrost soils are typically thinner than yedoma deposits (Ping et al., 2008; Tarnocai et al., 2009; Kanevskiy et al., 2011).

The relationship between ebullition, dissolved CH_4 concentration, and lake type (Fig. 6) also indicates that ebullition seeps releasing CH_4 produced deep in thaw bulbs contribute more to CH_4 cycling in yedoma lakes than in non-yedoma lakes. Yedoma lakes, which had a higher density of ebullition seeps than non-yedoma lakes (Sect. 3.2), had both higher volumes of CH_4-rich bubbles impeded by lake ice and higher concentrations of dissolved CH_4 in the lake water in winter (Fig. 6a, $r_s = 0.72$). Based on Greene et al. (2014), in which 93 % of dissolved CH_4 in the water column in winter originated from CH_4 dissolution from ebullition bubbles trapped by lake ice, we attribute the higher concentrations of dissolved CH_4 in the yedoma study lakes to the process of CH_4 dissolution from ice-trapped bubbles. Modeling results, which showed that approximately 80 % of CH_4 in bubbles trapped by lake ice in our study lakes dissolved into the water column, support this conclusion. Other important processes that would also control dissolved CH_4 concentrations in lake water are diffusion from sediments and CH_4 oxidation. Given the thicker CH_4-producing sediment package beneath yedoma lakes, we would expect diffusion of dissolved CH_4 from yedoma lakes to be higher than that of non-yedoma lakes. Ex situ incubations by Martinez-Cruz et al. (2015) on a subset of our Alaska study lakes also showed that yedoma lakes had higher CH_4 oxidation potentials, owing in large part to higher concentrations of the dissolved CH_4 substrate in these lakes. Compared to winter, the weaker correlation between dissolved CH_4 and direct ebullition in summer (Fig. 6b, $r_s = 0.42$) has several potential explanations. First, in summer, ebullition bubbles escape directly to the atmosphere, so the dissolved CH_4 stock of the water column is not supplied from ice-trapped bubble dissolution like it is in winter unless residual winter-dissolved bubble CH_4 remains in the water column in summer. Second, dissolved CH_4 diffusing from lake sediments in summer may be more immediately oxidized by aerobic CH_4 consumption since O_2 is more available in lake water from atmospheric diffusion and autochthonous primary production. Finally, higher SRP, TN, and Chl *a* concentrations in yedoma lakes (Table 1) suggests primary production in yedoma lakes may contribute relatively more substrate to methanogenesis in surface sediments. CH_4 produced in surface sediments more readily escapes to the water column via diffusion than CH_4 produced in thaw bulbs, which preferentially escapes by ebullition (Tan et al., 2014). Higher diffusion from surface sediments would support higher concentrations of dissolved CH_4 in lake water, a process that can be independent of ebullition from thaw bulbs in summer. This explanation is supported by 2 times higher summer diffusion emissions from yedoma lakes compared to non-yedoma lakes (Table 2), despite higher observed CH_4 oxidation potentials in yedoma lakes vs. non-yedoma lakes (Martinez-Cruz et al., 2015).

CO_2 diffusion, which was ~ 100 and 92 % of total annual CO_2 emissions from yedoma and non-yedoma lakes, respectively, was 6 times higher on average in yedoma lakes than in non-yedoma lakes. Potential explanations include enhanced CO_2 production associated with yedoma organic matter decomposition, photooxidation of the large DOC pool observed in the mixotrophic yedoma lakes, and potentially higher rates of CH_4 oxidation in yedoma lakes (Martinez-Cruz et al., 2015) generating more CO_2 in the lake water columns. The higher DOC content of yedoma lakes would favor CO_2 production; however, DOC quality has also been observed to be an important control over CO_2 emissions from northern lakes (Kortelainen et al., 2006). Vonk et al. (2013) recently showed that Pleistocene-aged DOC mobilized in stream water draining yedoma outcrops is exceptionally biolabile among contemporary fluvial systems in the Arctic. This suggests that yedoma-derived DOC in lakes may be more easily decomposed than non-yedoma DOC. Finally, possible differences in watershed sizes draining into lakes could also influence CO_2 concentrations in lakes and diffusion emissions since terrestrial dissolved inorganic carbon often dominates lake CO_2 pools (Kling et al., 1992; Battin et al., 2009; Tranvik et al., 2009). While Kortelainen et al. (2013) found lake water NO_3^- concentrations in Finnish lakes to control the ratio of terrestrially derived CO_2 emissions from lakes versus long-term carbon sequestration in lake sediments, we found no relationship between CO_2 emissions and NO_3^- concentrations. Since we did not study long-term carbon sequestration or the other aforementioned processes, and since our calculations contain uncertainty associated with the assumption that single-day measurements of dissolved CO_2 and CH_4 in lakes represent the mean flux for the entire open-water period, further research is needed to validate these hypotheses in the Alaskan lakes.

4.3 Dissolved CH_4 and O_2 dynamics

Dissolved O_2 concentration is a useful parameter for predicting the CH_4 concentrations in Alaskan lakes. The inverse relationship observed between CH_4 and O_2 concentration in lake water (Fig. 5) suggests physical and biological processes govern the availability of these compounds to different degrees in various lakes.

There are several possible explanations for the pattern of seasonally higher dissolved CH_4 and lower O_2 concentrations in winter among lakes (Fig. 5): (1) ice cover inhibits O_2 transfer from the atmosphere into the water column (White et al., 2008); (2) primary production in lakes declines as day length shortens (White et al., 2008; Clilverd et al., 2009); (3) snow cover impedes light transfer, further extinguishing photosynthesis beneath the ice (Welch et al., 1987; Clilverd et

al., 2009); and, finally, (4) aerobic microorganisms consume residual O_2 in the water beneath the ice (Bellido et al., 2009; Clilverd et al., 2009). The resulting anoxic conditions facilitate anaerobic processes like methanogenesis and decrease methanotrophy (Dunfield et al., 1993). All the while, CH_4 is emitted from lake sediments throughout winter via diffusion and seep ebullition. Many ebullition bubbles are impeded by lake ice, leading to dissolution of CH_4 from bubbles and an increase in dissolved CH_4 concentration. In summer, the lack of ice cover allows CH_4 in bubbles to be released directly to the atmosphere without partially dissolving in the lake water column. This explains in part the lower CH_4 concentrations in lake water in summer (Greene et al., 2014). Furthermore, the O_2 concentration in lake water increases in summer by gas exchange with the atmosphere and by primary production in lakes (Fig. 5b). As a result, a fraction of dissolved CH_4 in lake water is emitted to the atmosphere, while methanotrophic activity, supported by elevated O_2 concentration, oxidizes another fraction (Martinez-Cruz et al., 2015).

In addition to the seasonal variations described above, a permafrost-type effect on dissolved CH_4 and O_2 patterns was also observed. While most of the non-yedoma lakes were well oxygenated during summer, yedoma lakes in interior Alaska had contrastingly lower O_2 concentrations and higher dissolved CH_4 concentrations beneath the thermocline. This suggests high methanogenic activity in sediments that fuels CH_4 oxidation in the water column. Aerobic methane oxidation together with other aerobic processes reduces O_2 concentration under the thermocline, where stratification limits O_2 ingress from superficial water layers.

Understanding the dynamics of dissolved CH_4 and O_2 in northern lakes also has relevance to the distribution of lake biota. Ohman et al. (2006) showed that CH_4 concentration in the water column is correlated with fish community composition in lakes, which is easily understood since CH_4 can be used as an indicator of anoxia and therefore correlated with the fish O_2 requirements.

4.4 Limnological and morphological patterns

Single linear regression analysis indicated that the best limnological predictors of CH_4 emissions in the Alaskan lakes were area, SecD, SRP, and TN, all of which are indicators of lake metabolism and morphology (Table 4). These findings are consistent with the patterns that explain lake CH_4 emissions in Michigan, Canada, Sweden, and Finland (Bastviken et al., 2004; Juutinen et al., 2009; Rasilo et al., 2015), suggesting that lake trophic state and organic matter quality, rather than carbon concentration alone, might play prevailing roles in CH_4 and CO_2 production and fluxes. The association between high CH_4 emissions and high nutrients and Chl *a* concentrations among yedoma lakes compared to non-yedoma lakes is consistent with the geographic patterns previously observed in Siberian lakes. Higher aquatic production observed in Siberian yedoma lakes compared to non-yedoma lakes in the same climate zone was attributed to fertilization of the yedoma lakes by nitrogen- and phosphorus-rich thawing yedoma permafrost (Walter Anthony et al., 2014). Positive relationships between lake nutrient status and CH_4 fluxes together with low or negative CO_2 fluxes observed in other northern lakes also suggested that lake trophy plays diverging roles in CH_4 and CO_2 fluxes (Del Giorgio et al., 1999; Lapierre and Del Giorgio, 2012). Nutrients can increase primary productivity that simultaneously fuels methanogenesis and draws down dissolved CO_2.

The negative correlation between CH_4 emissions and lake area indicates that small lakes had higher total annual CH_4 emissions. This finding is driven by yedoma lakes, which were on average much smaller and tended to develop more noticeable anaerobic hypolimnia than non-yedoma lakes (Table 1, Fig. 5; Supplement Fig. B). This finding is also consistent with lake CH_4 emission patterns in other regions whereby smaller lakes have higher CH_4 emissions due to a stronger relative contribution of littoral organic matter to whole-lake methanogenesis (Bastviken et al., 2004; Juutinen et al., 2009; Rasilo et al., 2015).

4.5 Climate warming impacts of Alaskan lake emissions

Previously, Kling et al. (1992) showed that tundra lakes near Toolik Field station emit CH_4 and CO_2 via diffusion. More recently, Walter Anthony et al. (2012) recognized the importance of CH_4 ebullition from ecological seeps (formed from recent microbial decomposition vs. geologic seeps releasing fossil CH_4) in Alaskan lakes ($0.75\,Tg\ CH_4\ yr^{-1}$); however, this represented the quantity of ebullition seep CH_4 released from sediments rather than the magnitude of atmospheric emissions. Since ebullition emission is partially impeded by lake ice in winter, and a fraction of CH_4 dissolved out of bubbles beneath ice is oxidized by microbes (Greene et al., 2014), ebullition emissions to the atmosphere are lower than what is released annually from sediments. This study is the first to consider multiple modes of emissions for CO_2 and CH_4 together, including the ice-bubble storage process, for a large number of Alaskan lakes spanning large geographic gradients. Scaling total annual CH_4 and CO_2 emissions observed among yedoma and non-yedoma lakes to the extent of these lake types in Alaska (Walter Anthony et al., 2012) ($44 \pm 17\,g\ CH_4\ m^{-2}\ yr^{-1} \times \sim 8800\,km^2$, yedoma lakes; $8 \pm 4\,g\ CH_4\ m^{-2}\ yr^{-1} \times \sim 41\,700\,km^2$, non-yedoma lakes), we estimate that yedoma and non-yedoma lakes emit a total of $0.72\,Tg\ CH_4\ yr^{-1}$ ($\sim 0.39\,Tg\ CH_4\ yr^{-1}$ from yedoma lakes, $0.33\,Tg\ CH_4\ yr^{-1}$ from non-yedoma lakes). This estimate of Alaskan lake emissions increases the previous estimate of Alaska's wetland ecosystem emissions ($3\,Tg\ CH_4\ yr^{-1}$; Zhuang et al., 2007), in which lakes were not included, by 24 %. Our estimate of lake CH_4 emission is conservative because it does not include background (non-

seep) ebullition or storage emissions associated with fall lake turnover events.

If we assume that our study lakes represent the CH_4 and CO_2 emission dynamics of all lakes in Alaska and account for the 34-fold stronger global warming potential of CH_4 vs. CO_2 over 100 years (GWP_{100}; Myhre et al., 2013), the impact on the climate based on CO_2-equivalent (CO_2-eq) emissions from yedoma lakes is $\sim 20\,Tg\ CO_2\text{-eq}\,yr^{-1}$ ($13\,Tg\ CO_2\text{-eq}\,yr^{-1}$ from CH_4 and $7\,Tg\ CO_2\,yr^{-1}$ from CO_2). For non-yedoma lakes, the total climate impact is $\sim 17\,Tg\ CO_2\text{-eq}\,yr^{-1}$ ($11\,Tg\ CO_2\text{-eq}\,yr^{-1}$ from CH_4 and $6\,Tg\ CO_2\,yr^{-1}$ from CO_2). These results have several important implications. First, CH_4 emissions have nearly twice the impact on climate as CO_2 emissions among all Alaskan lakes. Second, the climate impacts of yedoma and non-yedoma lakes in Alaska due to carbon greenhouse gas emissions are approximately equal, despite yedoma lakes comprising less than one-fifth of the total lake area in Alaska. The disproportionately large climate impact of CH_4 emissions from yedoma lakes is due in large part to thaw of deep, organic-rich yedoma permafrost beneath these lakes; however, higher concentrations of total nitrogen, soluble reactive phosphorus, and chlorophyll *a* in these lakes suggest enhanced primary production in the lakes, which can also fuel decomposition and methanogenesis, as recently demonstrated in Siberia (Walter Anthony et al., 2014). Based on relationships observed in Finnish lakes, it is possible that shifts in nitrate availability could also control the long-term patterns of terrestrially derived CO_2 emission versus carbon sequestration by our study lakes as well.

5 Conclusions

Total annual CH_4 and CO_2 emissions were dominated by ebullition and diffusion, respectively; however, the climate warming impact of CH_4 emissions was twice that of CO_2. Our 40 study lakes spanned large gradients of physicochemical properties and geography in Alaska. We attribute the 6-fold higher CH_4 and CO_2 emissions observed in thermokarst lakes formed in icy, organic-rich yedoma permafrost in interior Alaska compared to non-yedoma lakes throughout the rest of Alaska to enhanced organic matter supplied from thawing yedoma permafrost, which is typically thicker than the organic-rich strata of non-yedoma soils. Higher total nitrogen, SRP, and Chl *a* concentrations in yedoma lakes suggest that higher primary production may also enhance organic substrate supply to decomposition and greenhouse gas production in these lakes. Consideration of multiple modes and seasonality of CH_4 and CO_2 emissions revealed that summer emissions were largest. However, winter and spring emissions of CH_4, including direct ebullition through holes in lake ice and the ice-bubble storage and release process, were also significant components of the annual CH_4 budget. Our results imply that regional assessments of lake CH_4 and CO_2 emissions in other parts of the pan-Arctic should take into account the myriad of emission modes and geographic characteristics, such as lake and permafrost types.

Appendix A: Methods

A1 Dissolved gas measurements

We used the headspace equilibration tunable diode laser spectroscopy (HE-TDLAS) technique, described in detail by Sepulveda-Jauregui et al. (2012), to measure the concentration of CH_4 dissolved in lake water. Briefly, we collected water samples using a Van Dorn bottle (WILDCO, Yulee, Florida, USA) and gently transferred 60 mL into three borosilicate vials (100 mL volume) using disposable polypropylene syringes for triplicate measurements. Vials were immediately sealed with butyl rubber stoppers and aluminum crimp caps. The vials containing the water samples were shaken vigorously for 10 s to transfer CH_4 from the water into the vials' headspace for subsequent measurement with the GasFinder 2.0.

In addition to HE-TDLAS, we also measured dissolved CH_4 and CO_2 in a subset of samples using the traditional headspace equilibration method by gas chromatography (Kling et al., 1992). Water samples (10 mL) collected with the Van Dorn bottle were transferred into 25 mL glass serum bottles and immediately sealed with butyl rubber stoppers and aluminum crimp caps. Serum bottles were stored upside down and frozen until laboratory analysis. In the laboratory, we thawed the samples to room temperature, shook bottles for 10 s to equilibrate headspace and water samples, and then measured CH_4 and CO_2 of the headspace by gas chromatography (Shimadzu GC-2014).

A2 Seep ebullition

GPS-mapped ebullition seeps were classified as A, B, C, and hotspot types, based on ice-bubble morphologies. This classification system has been described in detail, with example photographs and bubble morphology classification criteria presented in multiple previous publications (Walter et al., 2006, 2008; Walter Anthony et al., 2010, 2013). Briefly, A-type ebullition seeps are relatively small clusters of ebullition bubbles in which individual bubbles stack on top of each other in the winter ice sheet without merging laterally. Due to progressively higher ebullition rates, individual bubbles of B-type seeps laterally merge into larger bubbles under the ice prior to freezing in ice. A- and B-type seeps produce low-gas-volume clusters of bubbles in lake ice with cluster diameters typically < 40 cm. The larger C-type seeps result in large (usually > 40 cm diameter) pockets of gas in ice separated vertically by ice layers containing few or no bubbles. Bubble-trap measurements showed that the solid ice layers in between the large gas pockets of C-type seeps represent periods of relative quiescence in between large ebullition events (Walter et al., 2006; Walter Anthony et al., 2010). Hotspot seeps have the greatest mean daily bubbling rates. The frequency of ebullition release from hotspot seeps and the associated convection in the water column created by rising bubble plumes can be strong enough to maintain ice-free holes in winter lake ice or ice-free cavities covered by thin layers of ice during cold periods.

Thirty-day averages of bubbling rates (mL gas seep^{-1} d^{-1}) were determined through bubble-trap measurements of seep fluxes and associated with seep classes for each Julian day of the year (Walter Anthony et al., 2010). This data set consists of $\sim 210\,000$ individual flux measurements made using submerged bubble traps placed over ebullition seeps year-round. These class-specific fluxes were applied to the whole-lake mean densities of seeps on lakes to derive estimates of bubble-release rates from lake bottom sediments indexed by Julian day. To determine mass-based estimates of CH_4 and CO_2 in ebullition bubbles, we applied lake-specific measurements of CH_4 and CO_2 bubble concentrations to the individual lakes where seep-bubble gases were collected and measured. Methods of bubble-trap gas collection and measurements were described in detail by Walter et al. (2008). We sampled with bubble traps and measured by gas chromatography the CH_4 and CO_2 compositions of seep ebullition bubbles collected from up to 246 individual ebullition events per lake. In lakes where few or no seep-bubble gas concentrations were determined, we applied mean values of CH_4 and CO_2 by seep class (Walter Anthony et al., 2010): A, 73 % CH_4, 0.51 % CO_2; B, 75 % CH_4, 0.40 % CO_2; C, 76 % CH_4, 0.55 % CO_2; hotspot, 78 % CH_4, and 0.84 % CO_2. Whole-lake mean ebullition was the sum of seep fluxes observed along an average of five 50 m long transects per lake (median of four transects per lake), divided by the total area surveyed. In a recent comparison of methods for quantifying ebullition, Walter Anthony and Anthony (2013) showed that when at least three 50 m transects per lake are used to quantify seep ebullition, the estimate of mean whole-lake ebullition is 4–5 times more accurate than the mean flux determined by placement of seventeen 0.2 m^2 bubble traps randomly distributed across lake surfaces.

The Supplement related to this article is available online at doi:10.5194/bg-12-3197-2015-supplement.

Author contributions. K. M. Walter Anthony and A. Sepulveda-Jauregui conceived of the study. A. Sepulveda-Jauregui and K. M. Walter Anthony wrote the manuscript. K. M. Walter Anthony, A. Sepulveda-Jauregui, K. Martinez Cruz, and F. Thalasso were responsible for field and lab work. A. Sepulveda-Jauregui conducted statistical analyses. S. Greene modeled ice-bubble storage emissions. All authors commented on the composition of the manuscript.

Acknowledgements. We thank T. Howe for lab assistance, P. Anthony for spatial analysis and maps, and A. Strohm and J. Heslop for field and lab assistance. A. Powell, C. Mulder, and the students of the 2013 Scientific Writing, Editing, and Revising in the Biological Sciences course (Biol. 604) provided valuable comments on the paper. Support for the study came from DOE DE-SC0006920, NSF OPP #1107892, NSF ARC #1304823, NASA #NNX11AH20G, and the USGS NIWR. Specific support to A. Sepulveda-Jauregui and K. Martinez-Cruz came from Semarnat-Conacyt 23661, 206621/203709, and 330197/233369.

Edited by: W. F. Vincent

References

Abril, G., Guerin, F., Richard, S., Delmas, R., Galy-Lacaux, C., Gosse, P., Tremblay, A., Varfalvy, L., Dos Santos, M. A., and Matvienko, B.: Carbon dioxide and methane emissions and the carbon budget of a 10-year old tropical reservoir (Petit Saut, French Guiana), Global Biogeochem. Cy., 19, G02024, doi:10.1029/2007JG000608, 2005.

Arp, C. D. and Jones, B. M.: Geography of Alaska lake districts: Identification, description, and analysis of lake-rich regions of a diverse and dynamic state: US Geological Survey Scientific Investigations Report in: U.S.G.S.S.I., Gibbs, B., Fabian-Marks, J., Richey, B. J., Rogers, L., Richey, B. J., and Wahlstrom, S., USA, 2008–5215, 1–40, 2009.

Arp, C. D., Jones, B. M., and Grosse, G.: Recent lake ice-out phenology within and among lake districts of Alaska, USA, Limnol. and Oceanogr., 58, 2013–2028, 2013.

Bastviken, D., Ejlertsson, J., and Tranvik, L.: Measurement of Methane Oxidation in Lakes: A Comparison of Methods, Environ. Sci. Technol., 36, 3354–3361, 2002.

Bastviken, D., Cole, J., Pace, M., and Tranvik, L.: Methane emissions from lakes: Dependence of lake characteristics, two regional assessments, and a global estimate, Global Biogeochem. Cy., 18, GB4009, doi:10.1029/2004GB002238, 2004.

Bastviken, D., Cole, J. J., Pace, M. L., and Van de Bogert, M. C.: Fates of methane from different lake habitats: Connecting whole-lake budgets and CH_4 emissions, J. Geophys. Res.-Biogeosci., 113, G02024, doi:10.1029/2007JG000608, 2008.

Bastviken, D., Tranvik, L. J., Downing, J. A., Crill, P. M., and Enrich-Prast, A.: Freshwater Methane Emissions Offset the Continental Carbon Sink, Science, p. 331, 2011.

Battin, T. J., Luyssaert, S., Kaplan, L. A., Aufdenkampe, A. K., Richter, A., and Tranvik, L. J.: The boundless carbon cycle, Nat. Geosci., 2, 598–600, 2009.

Bellido, J. L., Tulonen, T., Kankaala, P., and Ojala, A.: CO_2 and CH_4 fluxes during spring and autumn mixing periods in a boreal lake (Paajarvi, southern Finland), J. Geophys. Res.-Biogeosci., 114, G04007, doi:10.1029/2009JG000923, 2009.

Boereboom, T., Depoorter, M., Coppens, S., and Tison, J.-L.: Gas properties of winter lake ice in Northern Sweden: implication for carbon gas release, Biogeosciences, 9, 827–838, doi:10.5194/bg-9-827-2012, 2012.

Borrel, G., Jezequel, D., Biderre-Petit, C., Morel-Desrosiers, N., Morel, J. P., Peyret, P., Fonty, G., and Lehours, A. C.: Production and consumption of methane in freshwater lake ecosystems, Res. Microbiol., 162, 832–847, 2011.

Brosius, L. S., Walter Anthony, K. M., Grosse, G., Chanton, J. P., Farquharson, L. M., Overduin, P. P., and Meyer, H.: Using the deuterium isotope composition of permafrost meltwater to constrain thermokarst lake contributions to atmospheric CH_4 during the last deglaciation, J. Geophys. Res.-Biogeosci.,117, G01022, doi:10.1029/2011JG001810, 2012.

Camacho, A.: On the occurrence and ecological features of deep chlorophyll maxima (DCM) in Spanish stratified lakes, Limentica, 25, 453–478, 2006.

Carlson, R. E.: Trophic State Index For Lakes, Limnol. Oceanogr., 22, 361–369, 1977.

Carlson, R. E. and Simpson, J.: A Coordinator's Guide to Volunteer Lake Monitoring Methods, North American Lake Management Society, 96 pp., 1996.

Casper, P., Maberly, S. C., Hall, G. H., and Finlay, B. J.: Fluxes of methane and carbon dioxide from a small productive lake to the atmosphere, Biogeochemistry, 49, 1–19, 2000.

Clilverd, H., White, D., and Lilly, M.: Chemical and physical controls on the oxygen regime of ice-covered arctic lakes and reservoirs, J. Am. Water Resour. As., 45, 500–511, 2009.

Cole, J. J. and Caraco, N. F.: Atmospheric exchange of carbon dioxide in a low-wind oligotrophic lake measured by the addition of SF, Limnol. Oceanogr., 43, 647–656, 1998.

Cole, J. J., Prairie, Y. T., Caraco, N. F., McDowell, W. H., Tranvik, L. J., Striegl, R. G., Duarte, C. M., Kortelainen, P., Downing, J. A., Middelburg, J. J., and Melack, J.: Plumbing the global carbon cycle: Integrating inland waters into the terrestrial carbon budget, Ecosystems, 10, 171–184, 2007.

Conrad, R., Claus, P., and Casper, P.: Stable isotope fractionation during the methanogenic degradation of organic matter in the sediment of an acidic bog lake, Lake Grosse Fuchskuhle, Limnol. Oceanogr., 55, 1932–1942, 2010.

Dean, W. E.: Determination of carbonate and organic matter in calcareous sediments and sedimentary rocks by loss on ignition; comparison with other methods, J. Sediment Res., 44, 242–248, 1974.

Del Giorgio, P., Cole, J. J., Caraco, N. F., and Peters, R. H.: Linking planktonic biomass and metabolism to net gas fluxes in northern temperate lakes, Ecology, 80, 1422–1431, 1999.

Downing, J. A., Prairie, Y. T., Cole, J. J., Duarte, C. M., Tranvik, L. J., Striegl, R. G., McDowell, W. H., Kortelainen, P., Caraco,

N. F., Melack, J. M., and Middelburg, J. J.: The global abundance and size distribution of lakes, ponds, and impoundments, Limnol. Oceanogr., 51, 2388–2397, 2006.

Duc, N. T., Crill, P., and Bastviken, D.: Implications of temperature and sediment characteristics on methane formation and oxidation in lake sediments, Biogeochemistry, 100, 185–196, 2010.

Dunfield, P., Knowles, R., Dumont, R., and Moore, T. R.: Methane production and consumption in temperate and sub-arctic peat soils-response to temperature and pH, Soil Biol. Biochem., 25, 321–326, 1993.

Dzyuban, A. N.: Dynamics of microbial oxidation of methane in the water of stratified lakes, Microbiology, 79, 822–829, 2010.

Gervais, F., Padisak, J., and Koschel, R.: Do light quality and low nutrient concentration favour picocyanobacteria below the thermocline of the oligotrophic Lake Stechlin?, J. Plankton Res., 19, 771–781, 1997.

Giblin, A., Luecke, C., Kling, G., and White, D.: Nutrient and chemical data for various lakes near Toolik Research Station, Arctic LTER, Summer 2009, Long Term Ecological Research Network, doi:10.6073/pasta/1b77f4c8d8cc250ce0f90bbb17d9c976, 2009.

Gow, A. J. and Langston, D.: Growth history of lake ice in relation to its stratigraphic, crystalline and mechanical structure, US Army, Corps of Engineers, Cold Regions Research and Engineering Laboratory, Hanover, New Hampshire, 24 pp., 1977.

Graneli, W., Lindell, M., and Tranvik, L.: Photo-oxidative production of dissolved inorganic carbon in lakes of different humic content, Limnol. Oceanogr., 41, 698–706, 1996.

Greene, S., Walter Anthony, K. M., Archer, D., Sepulveda-Jauregui, A., and Martinez-Cruz, K.: Modeling the impediment of methane ebullition bubbles by seasonal lake ice, Biogeosciences, 11, 6791–6811, doi:10.5194/bg-11-6791-2014, 2014.

Gregory-Eaves, I., Smol, J. P., Finney, B. P., Lean, D. R. S., and Edwards, M. E.: Characteristics and variation in lakes along a north-south transect in Alaska, Arch. Hydrobiol., 147, 193–223, 2000.

Grosse, G., Jones, B., and Arp., C.: Thermokarst lakes, drainage, and drained basins, Treatise Geomorph., 8, 325–353, 2013.

Guerin, F. and Abril, G.: Significance of pelagic aerobic methane oxidation in the methane and carbon budget of a tropical reservoir, J. Geophys. Res.-Biogeosci., 112, G03006, doi:10.1029/2006JG000393, 2007.

Haberman, J. and Haldna, M.: Indices of zooplankton community as valuable tools in assessing the trophic state and water quality of eutrophic lakes: long term study of Lake Vortsjarv, J. Limnol., 73, 263–273, 2014.

Jorgenson, T., Yoshikawa, K., Kanevskiy, M., Shur, Y., Romanovsky, V., Marchenko, S., Grosse, G., Brown, J., and Jones, B.: Permafrost Characteristics of Alaska, Institute of Northern Engineering, University of Alaska Fairbanks NICOP, University of Alaska Fairbanks, USA, 2008.

Juutinen, S., Rantakari, M., Kortelainen, P., Huttunen, J. T., Larmola, T., Alm, J., Silvola, J., and Martikainen, P. J.: Methane dynamics in different boreal lake types, Biogeosciences, 6, 209–223, doi:10.5194/bg-6-209-2009, 2009.

Kanevskiy, M., Shur, Y., Fortier, D., Jorgenson, M. T., and Stephani, E.: Cryostratigraphy of late Pleistocene syngenetic permafrost (yedoma) in northern Alaska, Itkillik River exposure, Quaternary Res., 75, 584–596, 2011.

Kankaala, P., Huotari, J., Peltomaa, E., Saloranta, T., and Ojala, A.: Methanotrophic activity in relation to methane efflux and total heterotrophic bacterial production in a stratified, humic, boreal lake, Limnol. Oceanogr., 51, 1195–1204, 2006.

Karlstrom, T. W., Coulter, H. W., Fernald, A. T., Williams, J. R., Hopkins, D. M., Pewe, T. L., Drewes, H., Muller, E. H., and Condon, W. H.: Surficial Geology of Alaska, U.S. Geological Survey Map, IMAP-357, http://pubs.er.usgs.gov/publication/i357, Interior, U.S.D.O., Alaska, USA, 1964.

Kessler, M. A., Plug, L., and Walter Anthony, K. M.: Simulating the decadal to millennial scale dynamics of morphology and sequestered carbon mobilization of two thermokarst lakes in N. W. Alaska, J. Geophys. Res., 117, G00M06, doi:10.1029/2011JG001796, 2012.

Kling, G. W.: Field and lab methods and protocols, Protocol version: v2.8, Kling Lab University of Michigan, 2010.

Kling, G. W., Kipphut, G. W., and Miller, M. C.: Arctic lakes and streams as gas conduits to the atmosphere – implications for tundra carbon budgets, Science, 251, 298–301, 1991.

Kling, G. W., Kipphut, G. W., and Miller, M. C.: The flux of CO_2 and CH_4 from lakes and rivers in arctic Alaska, Hydrobiologia, 240, 23–36, 1992.

Kortelainen, P., Rantakari, M., Huttunen, J. T., Mattsson, T., Alm, J., Juutinen, S., Larmola, T., Silvola, J., and Martikainen, P. J.: Sediment respiration and lake trophic state are important predictors of large CO_2 evasion from small boreal lakes, Glob. Change Biol., 12, 1554–1567, 2006.

Kortelainen, P., Rantakari, M., Pajunen, H., Mattsson, T., Juutinen, S., Larmola, T., Alm, J., Silvola, J., and Martikainen, P. J.: Carbon evasion/accumulation in boreal lakes is linked to nitrogen, Global Biogechem. Cy., 27, 363–374, 2013.

Langer, M., Westermann, S., Walter Anthony, K., Wischnewski, K., and Boike, J.: Frozen ponds: production and storage of methane during the Arctic winter in a lowland tundra landscape in northern Siberia, Lena River delta, Biogeosciences, 12, 977–990, doi:10.5194/bg-12-977-2015, 2015.

Lapierre, J. F. and Del Giorgio, P. A.: Geographical and environmental drivers of regional differences in the lake pCO_2 vs. DOC relationship across northern landscapes, J. Geophys. Res., 117, G03015, doi:10.1029/2012JG001945, 2012.

Lofton, D. D., Whalen, S. C., and Hershey, A. E.: Effect of temperature on methane dynamics and evaluation of methane oxidation kinetics in shallow Arctic Alaskan lakes, Hydrobiologia, 721, 209–222, 2014.

Maberly, S. C., Barker, P. A., Stott, A. W., and De Ville, M. M.: Catchment productivity controls CO_2 emissions from lakes, Nat. Clim. Change, 3, 391–394, 2013.

Madigan, M. T., Martinko, J. M., Dunlap, P. V., and Clark, D. P.: Brock biology of microorganisms, 12th Edn. Pearson education, 2009.

Marotta, H., Pinho L., Bastviken D., Tranvik L. J., and Enrich-Prast A.: Greenhouse gas production in low-latitude lake sediments responds strongly to warming, Nat. Clim. Change, 4, 467–470, 2014.

Martens, C. S., Kelley, C. A., Chanton, J. P., and Showers, W. J.: Carbon and hydrogen isotopic characterization of methane from

wetlands and lakes of the Yukon-Kuskokwim Delta, Western Alaska, J. Geophys. Res.-Atmos., 97, 16689–16701, 1992.

Martinez-Cruz, K., Sepulveda-Jauregui, A., Walter Anthony, K. M., and Thalasso, F.: Latitudinal and seasonal variation of aerobic methane oxidation in Alaskan lakes, Biogeosciences Discuss., in press, 2015.

Michmerhuizen, C. M., Striegl, R. G., and McDonald, M. E.: Potential methane emission from north-temperate lakes following ice melt, Limnol. Oceanogr., 41, 985–991, 1996.

Myhre, G., Shindell, D., Breon, F. M., Collins, W., Fuglestvedt, J., Huang, J., Koch, D., Lamarque, J. F., Lee, D., Mendoza, B., Nakajima, T., Robock, A., Stephens, G., Takemura, T., and Zhang, H.: Anthropogenic and Natural Radiative Forcing, in: Climate Change 2013: The Physical Science Basis, Contribution of Working Group I to the Fifth Assessment Report of the Intergovernmental Panel on Climate Change, Cambridge University Press, Cambridge, United Kingdom and New York, NY, USA, 2013.

National Institute of Standards and Technology (NIST): NIST chemistry Web book, 2011.

Ohman, J., Buffam, I., Englund, G., Blom, A., Lindgren, E., and Laudon L.: Associations between water chemistry and fish community composition: a comparison between isolated and connected lakes in northern Sweden, Freshwater Biol., 51, 510–522, 2006.

Ortiz-Llorente, M. J. and Alvarez-Cobelas, M.: Comparison of biogenic methane emissions from unmanaged estuaries, lakes, oceans, rivers and wetlands, Atmos. Environ., 59, 328–337, 2012.

Phelps, A. R., Peterson, K. M., and Jeffries, M. O.: Methane efflux from high-latitude lakes during spring ice melt, J. Geophys. Res.-Atmos., 103, 29029–29036, 1998.

Ping, C. L., Michaelson, G. J., Jorgenson, M. T., Kimble, J. M., Epstein, H., Romanovsky, V. E., and Walker, D. A.: High stocks of soil organic carbon in the North American Arctic region, Nat. Geosci., 1, 615–619, 2008.

Rasilo, T., Prairie, Y. T., and Del Giorgio, P. A.: Large-scale patterns in summer diffusive CH_4 fluxes across boreal lakes, and contribution to diffusive C emissions, Glob. Change Biol., 21, 1124–1139, 2015.

Repo, M. E., Huttunen, J. T., Naumov, A. V., Chichulin, A. V., Lapshina, E. D., Bleuten, W., and Martinkainen, P. J.: Release of CO_2 and CH_4 from small wetland lakes in western Siberia, Tellus B, 59, 788–796, 2007.

Schulz, S., Matsuyama, H., and Conrad, R.: Temperature dependence of methane production from different precursors in a profundal sediment (Lake Constance), Fems Microb. Ecol., 22, 207–213, 1997.

Semiletov, I. P., Pipko, II, Pivovarov, N. Y., Popov, V. V., Zimov, S. A., Voropaev, Y. V., and Daviodov, S. P.: Atmospheric carbon emission from North Asian Lakes: A factor of global significance, Atmos. Environ., 30, 1657–1671, 1996.

Sepulveda-Jauregui, A., Martinez-Cruz, K., Strohm, A., Walter Anthony, K. M., and Thalasso, F.: A new method for field measurement of dissolved methane in water using infrared tunable diode laser absorption spectroscopy, Limnol. Oceanogr.-Meth., 10, 560–567, 2012.

Smith, L. C., Sheng, Y. W., and MacDonald, G. M.: A first pan-Arctic assessment of the influence of glaciation, permafrost, topography and peatlands on northern hemisphere lake distribution, Permafrost Periglac., 18, 201–208, 2007.

Tan, Z., Zhuang, Q., and Walter Anthony, K. M.: Modeling methane emissions from arctic lakes: model development and site-level study, J. Adv. Model. Earth Sy., 7, doi:10.1002/2014MS000344, 2015.

Tarnocai, C., Canadell, J.G., Schuur, E.A.G., Kuhry, P., Mazhitova, G., and Zimov, S.: Soil organic carbon pools in the northern circumpolar permafrost region, Global Biogeochem. Cy., 23, GB2023, doi:10.1029/2008GB003327, 2009.

Tedford, E. W., MacIntyre1, S., Miller, S. D., and Czikowsky, M. J.: Similarity scaling of turbulence in a temperate lake during fall cooling, J. Geophys. Re.-Oceans, 119, 4689–4713, 2014.

Tranvik, L. J., Downing, J. A., Cotner, J. B., Loiselle, S. A., Striegl, R. G., Ballatore, T. J., Dillon, P., Finlay, K., Fortino, K., Knoll, L. B., Kortelainen, P. L., Kutser, T., Larsen, S., Laurion, I., Leech, D. M., McCallister, S. L., McKnight, D. M., Melack, J. M., Overholt, E., Porter, J. A., Prairie, Y., Renwick, W. H., Roland, F., Sherman, B. S., Schindler, D. W., Sobek, S., Tremblay, A., Vanni, M. J., Verschoor, A. M., von Wachenfeldt, E., and Weyhenmeyer, G. A.: Lakes and reservoirs as regulators of carbon cycling and climate, Limnol. Oceanogr., 54, 2298–2314, 2009.

Utsumi, M., Nojiri, Y., Nakamura, T., Nozawa, T., Otsuki, A., Takamura, N., Watanabe, M., and Seki, H.: Dynamics of dissolved methane and methane oxidation in dimictic Lake Nojiri during winter, Limnol. Oceanogr., 43, 10–17, 1998.

Vonk, J. E., Mann, P. J., Davydov, S., Davydova, A., Spencer, R. G. M., Schade, J., Sobzak, W. V., Zimov, N., Zimov, S., Bulygina, E., Eglington, T. I., and Holmes, R. M. High biolability of ancient permafrost carbon upon thaw, J. Geophys. Res. Lett., 40, 2689–2693, 2013.

Walter, K. M., Zimov, S. A., Chanton, J. P., Verbyla, D., and Chapin, F. S.: Methane bubbling from Siberian thaw lakes as a positive feedback to climate warming, Nature, 443, 71–75, 2006.

Walter, K. M., Engram, M., Duguay, C. R., Jeffries, M. O., and Chapin, F. S.: The potential use of synthetic aperture radar for estimating methane ebullition from Arctic lake, J. Am. Water Resour. As., 44, 305–315, 2008.

Walter Anthony, K. M., Vas, D. A., Brosius, L., Chapin, F. S., Zimov, S. A., and Zhuang, Q. L.: Estimating methane emissions from northern lakes using ice-bubble surveys, Limnol. Oceanogr.-Meth., 8, 592–609, 2010.

Walter Anthony, K. M., Anthony, P., Grosse, G., and Chanton, J.: Geologic methane seeps along boundaries of Arctic permafrost thaw and melting glaciers, Nat. Geosci., 5, 419–426, 2012.

Walter Anthony, K. M. and Anthony, P.: Constraining spatial variability of methane ebullition seeps in thermokarst lakes using point process models, J. Geophys. Res.-Biogeosci., 118, 1015–1034, 2013.

Walter Anthony, K. M., Zimov S. A., Grosse, G., Jones, M. C., Anthony, P., Chapin III, F. S., Finlay, J. C., Mack, M. C., Davydov, S., Frenzel, P., and Frolking S.: A shift of thermokarst lakes from carbon sources to sinks during the Holocene epoch, Nature, 511, 452–456, 2014.

Welch, H. E., Legault, J. A., and Bergmann, M. A.: Effects of snow and ice on the annual cycles of heat and light in Saqvaqjuac Lakes, Can. J. Fish. Aquat. Sci., 44, 1451–1461, 1987.

Weyhenmeyer G. A. and Karlsson, J.: Nonlinear response of dissolved organic carbon concentrations in boreal lakes to increasing temperatures, Limnol. Oceanogr., 54, 2513–2519, 2009.

Weyhenmeyer, G. A., Kortelainen, P, Sobek, S., Muller, R., and Rantakari, M.: Carbon Dioxide in Boreal Surface Waters: A Comparison of Lakes and Streams, Ecosystems, 15, 1295–1307, 2012.

West, J. J. and Plug, L. J.: Time-dependent morphology of thaw lakes and taliks in deep and shallow ground ice, J. Geophys. Res.-Earth Surf., 113, F01009, doi:10.1029/2006JF000696, 2008.

Wetzel, R. G.: Limnology: Lake and River Ecosystems. Academic Press Elsevier, San Diego, California, USA, 2001.

White, D. M., Clilverd, H. M., Tidwell, A. C., Little, L., Lilly, M. R., Chambers, M., and Reichardt, D.: A tool for modeling the winter oxygen depletion rate in arctic lakes, J. Am. Water Resour. As., 44, 293–304, 2008.

Williamson, C. E., Morris, D. P., Pace, M. L., and Olson, O. G.: Dissolved organic carbon and nutrients as regulators of lake ecosystems: Resurrection of a more integrated paradigm, Limnol. Oceanogr., 44, 795–803, 1999.

Yvon-Durocher, G., Allen, A. P., Bastviken, D., Conrad, R., Gudasz, C., St-Pierre, A., Thanh-Duc, N., and Del Giorgio, P. A.: Methane fluxes show consistent temperature dependence across microbial to ecosystem scales, Nature, 507, 488–491, 2014.

Zhuang, Q., Melillo, J. M., McGuire, A. D., Kicklighter, D. W., Prinn, R. G., Steudler, P. A., Felzer, B. S., and Hu, S.: Net emissions of CH_4 and CO_2 in Alaska: Implications for the region's greenhouse gas budget, Ecol. Appl., 17, 203–212, 2007.

Zimov, S. A., Voropaev, Y. V., Semiletov, I. P., Davidov, S. P., Prosiannikov, S. F., Chapin, F. S., Chapin, M. C., Trumbore, S., and Tyler, S.: North Siberian lakes: A methane source fueled by Pleistocene carbon, Science, 277, 800–802, 1997.

Zimov, S. A., Voropaev, Y. V., Davydov, S. P., Zimova, G. M., Davydova, A. I., Chapin III, F. S., and Chapin, M. C.: Flux of methane from north Siberian aquatic systems: Influence on atmospheric methane, in: Permafrost Response on Economic Development, Environmental Security and Natural Resources, NATO Science Series 2, 76, edited by: Paepe, R. and Melnikov, V. P., Kluwer Academic Publishers, Dordrecht, Netherlands; Boston, Massachusetts, USA, 511–524, 2001.

Zimov, S. A., Schuur, E. A. G., and Chapin III, F. S.: Permafrost and the Global Carbon Budget, Science, 312, 1612–1613, 2006.